Review

A Comprehensive Review of Post-Synthesis Modification Techniques of Zeolite Y and Their Influence on Properties

Abdullah Alsaban , Waheed Al-Masry , Sajjad Haider , Asif Mahmood , Abdulrahman Bin Jumah *

Posted Date: 30 December 2025

doi: 10.20944/preprints202512.2606.v1

Keywords: zeolite Y; FAU framework; modification techniques; hierarchical porosity; catalysis; adsorption

Review

A Comprehensive Review of Post-Synthesis Modification Techniques of Zeolite Y and Their Influence on Properties

Abdullah Alsaban, Waheed Al-Masry, Sajjad Haider, Asif Mahmood and Abdulrahaman Bin Jumah *

Department of Chemical Engineering, King Saud University, P.O. Box 800 Riyadh 11421, Saudi Arabia

* Correspondence: abinjumah@ksu.edu.sa

Abstract

Zeolite Y has been considered as one of the most versatile materials that are used in catalysis, adsorption, and separation. However, its inherent microporosity often impedes the diffusion of reactants and products, thus constraining overall performance. This review systematically investigates the major post-synthetic modification strategies intended to mitigate these limitations and to refine the structural and physicochemical properties of zeolite Y. Particular focus is placed on the mechanisms and structural consequences of dealumination, desilication, ion exchange, and surface functionalization, each of which uniquely influences acidity, porosity, and framework stability. The synergistic combination of dealumination and desilication is especially highlighted for its capacity to generate hierarchical structures containing mesoporosity with optimal acidity robustness. Recent developments that integrate the use of microwave and ultrasound-enhanced methods are considered sustainable and energy-efficient solutions that offer accurate control over the framework transformation and shorten processing times. These post-synthetic advancements have led to hierarchical, multifunctional zeolite Y materials that show high levels of catalytic activity, enhanced adsorption capacity, and improved selectivity over a wide range of industrially related reactions. This review concludes how such modification techniques expand the functional range of zeolite Y, thereby enabling its use in new areas of application, including CO_2 capture, biofuels production, and environmentally friendly catalytic processes. Future perspectives emphasize ongoing refinement of structure-function relationships, scalability of processes, and integration of modification methodologies to reinforce zeolite Y's pivotal role in sustainable chemical manufacturing.

Keywords: zeolite Y; FAU framework; modification techniques; hierarchical porosity; catalysis; adsorption

1. Introduction

1.1. Historical Background

The name "zeolite" was first used by Swedish geologist Axel Cronstedt in 1756. He combined the Greek words Zeo (to boil) and Lithos (stone). Cronstedt noticed that the material released large amounts of steam upon heating, due to water previously adsorbed by the substance [1]. Substantial advancements in the scientific understanding of zeolites were hindered until the year 1840, when Damour elucidated their reversible hydration and dehydration characteristics [2]. In 1858, the cation-exchange characteristics of naturally occurring zeolites, such as natrolite and chabazite, were established [3], followed by the synthesis of the first artificial zeolite, known as levyne, by Sainte Claire Deville in 1862 [4]. The first attempts regularly met obstacles in consistency because of a lack of detailed description, causing continuous arguments about their authenticity. Nevertheless, scholarly interest in zeolites intensified, particularly after the findings of Friedel (1896) and Grandjean

 doi:10.20944/preprints202512.2606.v1

(1909), who reported the adsorption of compounds other than water, which culminated in the 1924 discovery of the molecular sieve effect by Weigel and Steinhoff [5–7]. This phenomenon was ultimately elucidated in the 1930s, when the structural porosity of zeolites was clarified, leading McBain in 1932 to introduce the concept of "molecular sieve" [8–11]. This advancement motivated Richard M. Barrer, now recognized as a pioneer in zeolite science, who embarked on comprehensive research regarding zeolite synthesis and separation methodologies, resulting in the production of synthetic analogs of both naturally occurring, including mordenite and chabazite, and innovative frameworks such as Q and P zeolites [12–17]. In 1949, Barrer pioneered the ammonium exchange method with subsequent calcination to yield protonic zeolites [18], and subsequently advanced the employment of tetraalkylammonium cations in synthesis [19–21], a technique that remains integral to this day [22–24]. His research garnered industrial attention, culminating in a partnership with Union Carbide in the United States that commenced in 1949. Robert M. Milton, a participant in this initiative, modified synthesis conditions to generate X and A zeolites [25,26], followed by the 1954 identification of zeolite Y by Donald W. Breck after joining Milton's team. Union Carbide then proceeded to expand the production and commercialize X and A zeolites in 1954, and further identified 24 additional zeolite species, thereby establishing their significance in industrial applications [25–30]. By the early 1960s, synthetic zeolites, particularly X and its modified variant Y, were employed by Mobil Oil Company in the hydrocarbons catalytic cracking, and by the 1970s, zeolites ZSM-5 and beta were introduced, while zeolite A began to be utilized in detergents, signifying the comprehensive industrial integration of these materials [31,32].

1.2. Description of Zeolite

Zeolites are minerals composed of crystalline aluminosilicates [33]. They can be described as a framework consisting of tetrahedrons of SiO_4 and AlO_4, which are interconnected at their vertices by a shared oxygen ion as shown in Figure 1.

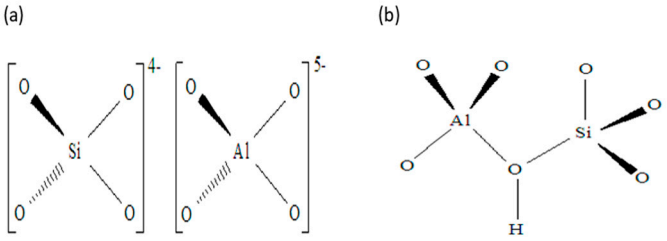

Figure 1. Tetrahedral configuration of SiO_4 and AlO_4 molecules (a) and the corresponding Si-O and Al-O bonds (b) that form unit blocks of a zeolite.

The introduction of a trivalent Al^{+3} ion through isomorphic substitution of Si^{+4} creates a negative charge within the lattice, necessitating compensation. The incorporation of cations, like as alkali, alkali-earth metals (e.g. Na^+, K^+ or Ca^{2+}), into the crystal structure neutralizes the negatively charged aluminum-containing tetrahedra. The voids between these tetrahedra, constituting channels within the structure, are naturally filled with water molecules [34–36]. Thus, the smallest zeolite structural unit can generally be described by the formula (1):

$$M_{x/n}.\left[(Al_2O_3)_x(SiO_2)_y\right].wH_2O \quad (1)$$

where M represents a hydrogen ion or a metal cation that balances the negative charge of the zeolite framework, x and y are the numbers of $[AlO_4]^{5-}$ and $[SiO_4]^{4-}$, n is the valence of the cation, and w is the amount of water present in the zeolite cavities. Moreover, the number of metal cations (e.g., Na^+) must match the total negative charge created by the silicon and aluminium ions, which carry charges of 4^+ and 3^+, respectively [37].

 doi:10.20944/preprints202512.2606.v1

Each tetrahedral TO_4 molecules (T represents either Al or Si atoms) are called primary building units (PBUs). These are then combined to form secondary building units (SBUs) that create basic structural polyhedral shapes such as cubes or truncated octahedrons (14-sided) (Figure 2) [38].

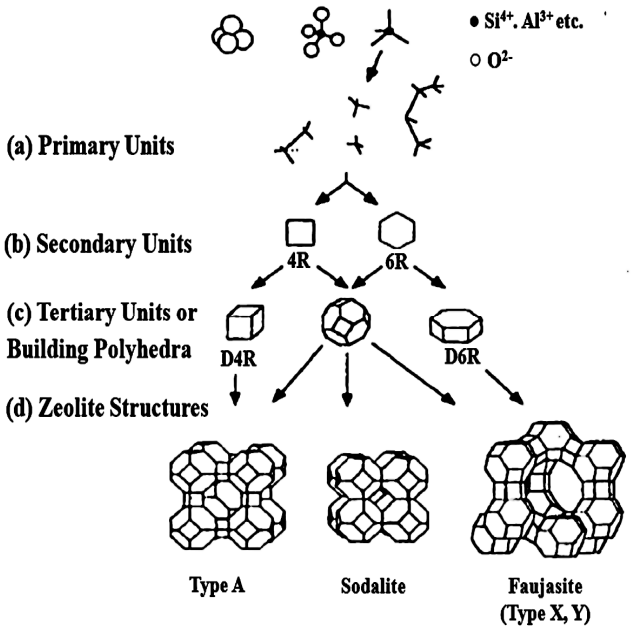

Figure 2. Synthesis pathways of three common zeolites from their basic structural building units [38].

Their structural and chemical properties make them essential in applications such as catalysis, adsorption, and separation. The unique pore architecture and acidity position them as powerful catalysts in industrial processes including cracking, isomerization, and alkylation, with modifications like ion exchange and metal impregnation enhancing performance for environmentally friendly chemical transformations [39]. Additionally, they are highly effective in catalytic oxidation processes, such as the thermal and photocatalytic decomposition of volatile organic compounds (VOCs) [40]. Also, their high surface and porosity make them excellent adsorbents, facilitating the targeted adsorption of contaminants from air and water for environmental remediation and energy conversion. Moreover, zeolites are extensively employed in separation processes in applications like chemical production, purification, and membrane technology for efficient gas and liquid separation due to their ability to selectively filter molecules by size and polarity [41,42].

Zeolite classification depends on various factors, including framework topology, the ratio of silicon to aluminum, and the characteristics of extra-framework cations [31]. Common examples of zeolite types include ZSM-5, Mordenite, and Y zeolites, each with its own distinct characteristics and applications (Figure 3). For instance, in terms of catalytic applications, ZSM-5 is renowned for its ability to selectively catalyze reactions based on shape and has found use for the catalytic cracking of hydrocarbons to produce high-octane gasoline [43,44]. On the other hand, Mordenite has been utilized in catalyzing key reactions such as alkylation, hydrocracking, reforming, hydro isomerization, dewaxing, and the synthesis of dimethylamines [45]. Y zeolites are broadly applied in fluid catalytic cracking due to their stability and acidic properties [46]. Therefore, A thorough knowledge of the different types of zeolites is crucial for tailoring them to specific industrial processes.

 doi:10.20944/preprints202512.2606.v1

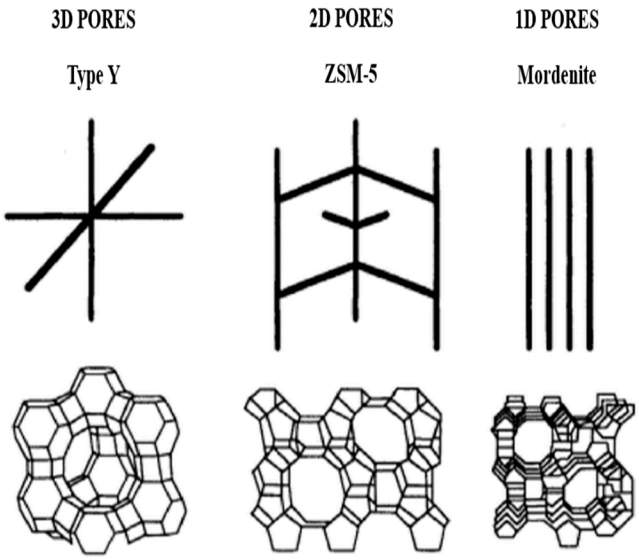

Figure 3. The structure dimensions of Y zeolite, ZSM-5, and Mordenite [38].

1.3. Zeolite Y

Zeolite Y possesses a three-dimensional microporous structure and inherent acidity, making it an invaluable tool in numerous applications [47]. It is most commonly used in industry as ultra-stable Y zeolite (USY), which is produced by steaming high Al zeolite Y, leading to a partial removal of framework Al and generating extra framework AL (EFAL) species that persist in solids and reside within the pores. This reduces the total amount of acid sites and improves the material's resistance to hydrothermal degradation [48,49].

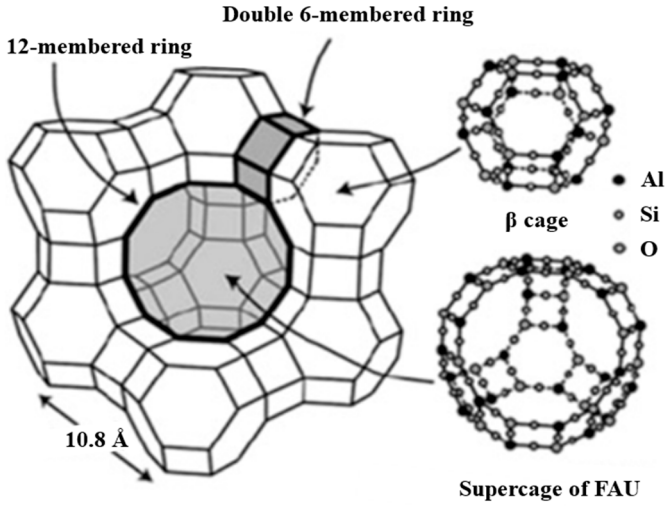

Figure 4. Schematic of the framework structure of Faujasite-type zeolites [50].

As illustrated in Figure 4, the structural design of Y-type zeolite, placed in the FAU zeolite category, includes three separate types of pores found in its crystal lattice: (a) the supercages that have a pore width of 0.74 nm and an inner space diameter of 1.2 nm (b) the sodalite cage, also called the β-cage, which offers a pore opening of 0.26 nm and an internal diameter of 0.66 nm and (c) the hexagonal prism which shows a pore opening that is reduced in size relative to the sodalite cage [51]. Therefore, its intrinsic micropores (<1 nm) give rise to the persistent challenge related to restricted accessibility and limited diffusion during catalysis and adsorption. For example, in terms of catalysis, the limited accessibility of active sites within the pore structure to the reactants and the reduced diffusion rate of the reaction products from the pore interior to the bulk media, resulting in low

 doi:10.20944/preprints202512.2606.v1

reaction conversion [52]. To overcome these limitations and fully unlock Y zeolite's potential, innovative approaches for improving its properties are essential. In this review, not only a comprehensive overview of the different methods of post-synthesis modification of Zeolite Y will be provided, but also an analysis of the impact of these modifications on the structure, physicochemical properties, and applications.

2. Types of Post-Synthesis Modifications

2.1. Dealumination Techniques

Dealumination of zeolites is a critical process aimed at enhancing their properties by removing aluminum from their frameworks [53]. Various techniques are used to dealuminate Y zeolite, like Acid treatments, steam treatment, and the use of chemical agents (Figure 5). Each method has its advantages and limitations, influencing the extent of aluminum removal and the resultant properties of the zeolite. For instance, Acid leaching is one of the most widely used methods for dealumination. Noted that it has been employed extensively in the zeolite industry, particularly for the preparation of USY zeolite, which is a powerful catalyst for oil cracking [54]. The mechanism of this technique involves an acid attack on negatively charged oxygen sites bonded to aluminum atoms. The process facilitates the extraction of aluminum from the zeolitic framework and typically results in an increase in the Si/Al ratio, which enhances the thermal stability of the zeolite [55]. As an example of this technique, the research by Buchori and Anggoro [56] that focused on modifying zeolite Y for the production of dimethyl ether from methanol dehydration. This study investigates zeolite Y dealumination using sulfuric acid solution at different temperatures and acid concentrations. The results showed that the zeolite Y catalyst that dealuminated at 50°C and acid concentration of 8.5 N exhibits higher activity in the synthesis of dimethyl ether compared to unmodified zeolite Y, with a methanol conversion of 76.07%. Maghfirah et al. [57] investigate the role of additives such as tetraalkylammonium (TAA) cations during acid leaching using oxalic acid (0.1,0.25, and 0.5 M), resulting in the protection of the zeolite framework, and enhancing the Si/Al ratio (from 3.4 to 12.6) while maintaining crystallinity. Moreover, the extent of dealumination is influenced by factors such as the pH of the acid solution and the rate of acid addition, which are crucial for optimizing the treatment conditions to retain crystallinity and enhance catalytic activity [58].

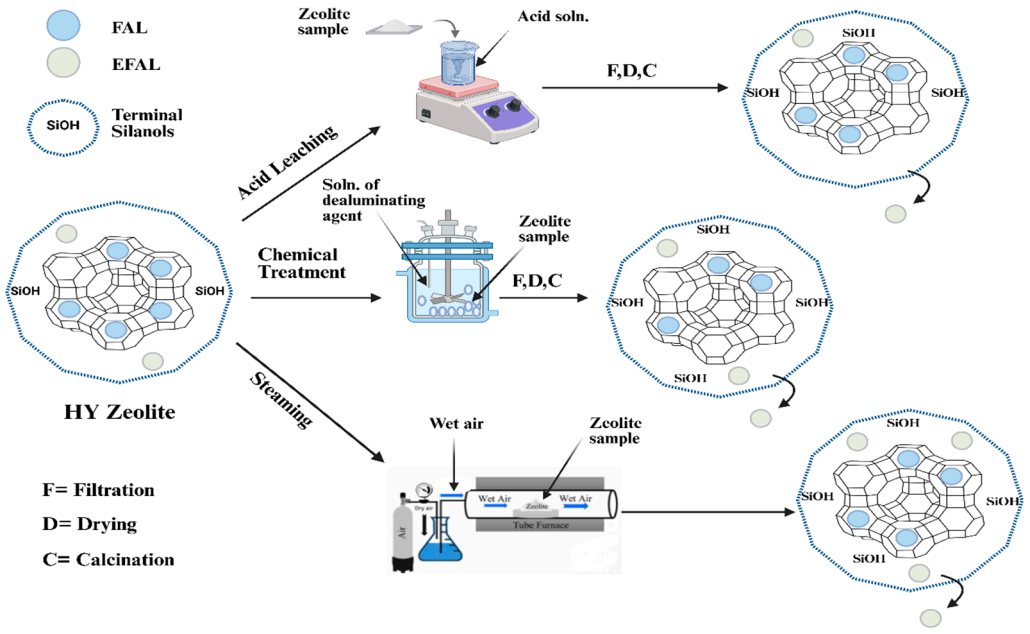

Figure 5. Schematic of the dealumination processes of zeolite Y (own elaboration based on Buchori and Anggoro [56], Kamimura et al. [59], Abdulridha et al. [60] and Lutz et al. [61]).

 doi:10.20944/preprints202512.2606.v1

Another technique that is closely similar to acid leaching is chemical treatment, which refers to the use of specific reagents such as citric acid, ammonium fluosilicate (AFS), ethylene diamine tetra acetic acid (EDTA), or other chelating agents that target aluminum atoms in the zeolite framework and extract them in a controlled manner [62,63]. These chemicals interact with the aluminum atoms, either forming complexes that can be washed away, e.g., in the case of AFS or EDTA or directly removing framework aluminum through substitution or ion-exchange processes [64]. It is distinguished from acid leaching by its high selectivity and minimizing framework damage and is often used when precise control of aluminum removal is needed for specific applications [65]. For instance, various modifications of USY zeolites were explored for enhancing their catalytic properties in hydrocracking reactions, primarily focusing on chemical dealumination modification. As outlined in their research, Qiao et al. [66] utilized citric acid and ammonium fluosilicate, Li et al. [67] employed citric acid and phosphoric acid, and Qiao et al. [68] centered their examination on malic nitric acid. These modifications resulted in enhanced hydrothermal stability, increased secondary pore volume, appropriate acidity distribution, and improved crystallinity, leading to superior performance compared to commercial catalysts. Furthermore, Qiao et al [69]. achieved hierarchical USY by post-treatment using EDTA-2Na and citric acid, which improved surface area and pore volume through both non-framework and framework dealumination mechanisms, ultimately enhancing mesoporosity and crystallinity. In addition, different types of zeolite Y including (Y, NH_4Y, HY, and NaY) were dealuminated by Hosseini et al [70] utilizing acetylacetone (as a chelating agent) and/or in the presence of ultrasound irradiation. The ultrasound technique has proven itself as an effective tool in increasing dealumination and it is attributed to the effective interaction between the zeolite particles and the chelating molecules, which generates cavitation and causes mechanical erosion of the solid, resulting in an efficient removal process as shown in Figure 6, where unit cell size clearly decreased when ultrasound is applied, indicating higher dealumination.

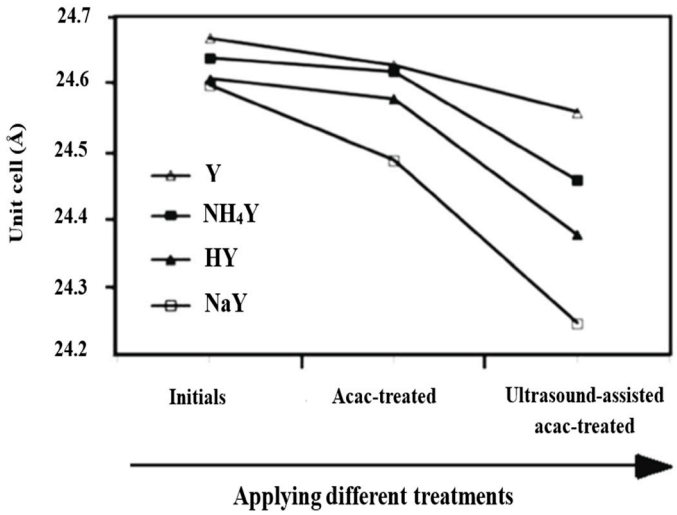

Figure 6. Unit cell size for the initials, acetylacetone-treated, and ultrasound-assisted acetylacetone-treated zeolite Y samples from XRD data [70].

The chemical dealumination can also enhance the adsorption capacity for larger molecules. Esmaeili et al. [71] conducted an acid, alkaline, and chemical treatment to improve the adsorption capacity of zeolite Y for dye removal from polluted water. They found that the treatment that gave considerable results was the chemical treatment using ammonium hexafluorosilicate (AHFS) as they prepared solutions with different concentrations of AHFS (4, 12, and 20%). The higher concentration of AHFS led to better adsorption results of rhodamine B (RB) dye, although it also risked damaging the zeolite's structure.

 doi:10.20944/preprints202512.2606.v1

On the other hand, Steam treatment, or hydrothermal dealumination, is a different dealumination technique that involves exposing zeolite Y to steam at high temperatures (typically between 500 and 700 °C) in the presence of air or oxygen. It causes hydrolysis of Al-O bonds that facilitate the removal of aluminum from the framework and their subsequent deposition as EFAL species [61]. Although many studies state that steaming is more efficient at high temperatures, and doing otherwise may cause the accumulation of these EFAL inside the pores blocking active sites [72], Agostini et al. [73] have a different opinion. They steam NH_4-Y zeolite to 600 °C and found that during heating from 510 to 600 °C only 5% of Al species is extracted, whereas 30-35% is removed during cooling from 227 to 177 °C. According to XAS, XRPD, and TG measurements, this is attributed to water molecules when they begin to repopulate the pores causing the dislodgement of Al from the zeolite structure. In addition, Studies have shown that steaming can lead to dramatically enhanced activity via the formation of stronger acid sites, particularly in low-silica zeolites [74]. However, the only disadvantage of this technique is that it is size-dependent, larger crystals (over 500 nm) can achieve higher Si/Al ratios, while smaller crystals may degrade under similar conditions. Therefore, in the case of smaller ones, other dealumination methods are recommended like chemical treatment (e.g. using AHFS) as it provides a gentler approach [75].

2.2. Desilication

Desilication is a method that specifically eliminates silicon from the zeolite framework, improving the material's porosity by generating mesopores while preserving the structure of the zeolite. Usually, zeolite Y is treated with alkaline solutions like sodium hydroxide (NaOH) to help in the specific removal of silicon atoms from the structure [76]. Figure 7 shows the steps of the desilication process of zeolite Y.

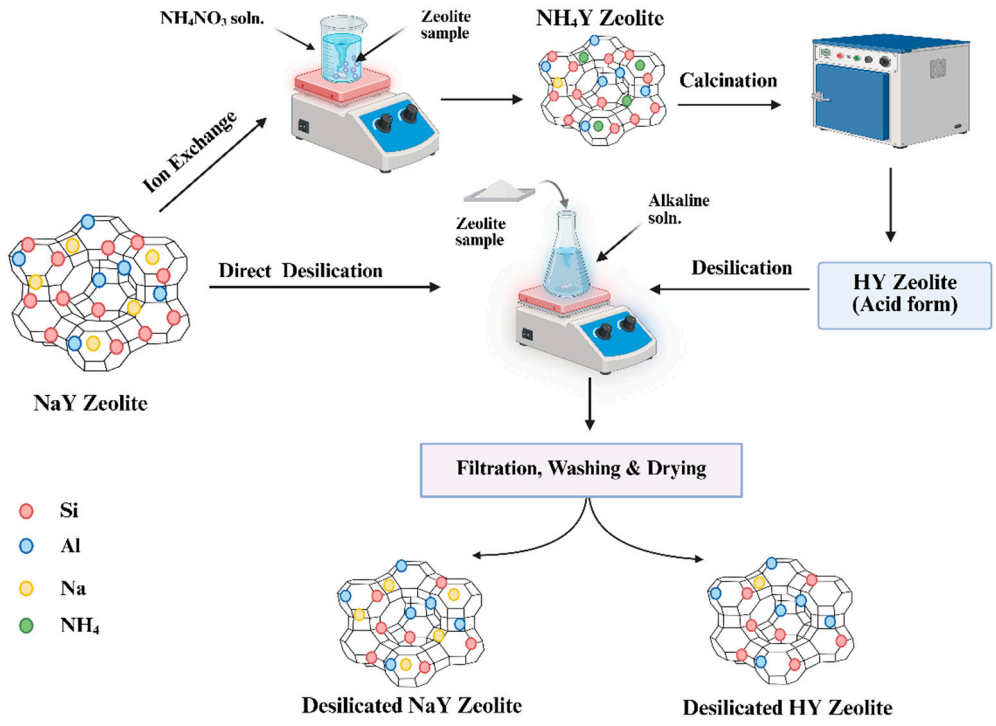

Figure 7. Schematic of the desilication process of zeolite Y(own elaboration based on Liang et al. [77], García et al. [78] and Dashtpeyma et al. [79]).

The desilication conditions, such as alkaline solution concentration, treatment duration, and Si/Al ratio, have a major impact on the porosity and acidity of zeolite Y. García et al. [78] stated that using NaOH solutions with a concentration of (0.05 to 0.20 M) for 15 minutes at room temperature is enough to induce effective mesoporosity in the range of (20–100 Å). Han et al. [80] used

 doi:10.20944/preprints202512.2606.v1

tetraalkylammonium hydroxide (TAAOH) as a desilication agent and found that a higher Si/Al ratio (i.e. 15-28) is optimal for controlled mesoporosity development while maintaining crystalline structure. However, it was found that the desilication of zeolites of high Si/Al ratio in alkali solutions leads to the removal of both Si and Al from the zeolite structure, but Si stays dissolved in the solution, while Al is reintroduced into the zeolite framework. The use of mild acid washing post-desilication can solve this issue as it has been shown to effectively remove residual aluminum species, thereby enhancing the overall performance of the modified zeolite Y [81].

In contrast, if zeolite Y has a low Si/Al ratio, a prior dealumination may be needed to raise the Si/Al ratio and improve the effectiveness of later desilication. For instance, Zhang et al. [82] performed post-synthesis chemical dealumination followed by desilication of the parent zeolite Y (with Si/Al ratio of 2.6). In this study, ultrasonic-assisted treatment was used in place of conventional alkaline treatment, showing a decrease in desilication time (5 min vs. 30 min, at the same conditions of 0.2 mol/L NaOH at 65°C) and enhancement in the specific external surface area and mesopore volume of the catalyst more than the conventional method. Similarly, Pagis et al. [83] performed pre-dealumination to NaY zeolite (Si/Al=2.5) with silicon tetrachloride ($SiCl_4$). Then, the dealuminated zeolite was acid-leached with a 0.1 M hydrochloric acid solution (HCl) to remove part of EFAl species deposited inside the pores that further raised the Si/Al to 37.7 before desilication with sodium aluminate ($NaAlO_3$) (Figure 8). The desilication was held with Al species to provide the crystals with an Al-rich surface and a Si-rich core, resulting in a hollow structure and hierarchical patterns. Mandela et al. [84] modified zeolite Y (Si/Al=5) using hydrochloric acid and/or sodium hydroxide treatment for catalytic hydrotreating of α-cellulose bio-oil. The results show that applying both HCl and NaOH treatment led to an increase of the zeolite Y average pore diameter, proving the effectiveness of this technique in creating mesoporosity in low Si/Al zeolite Y. Moreover, Li et al. [47] found that excessive aluminum content can hinder the desilication process. This results in inadequate mesopore development. Hence, it is necessary to strike a delicate balance between these two processes in order to obtain the desired structural properties.

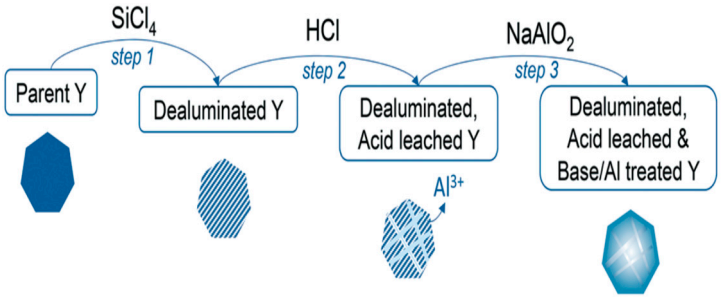

Figure 8. A schematic diagram of the fabrication process for hollow zeolite Y with three phases [83].

The addition of surfactants as templating agents during alkaline treatment like tetra propylammonium (TPA^+) and cetyltrimethylammonium (CTA^+) is a significant factor in the desilication process and helps in the formation of mesopores [85,86]. Verboekend et al. [87] examine the influence of TPA^+ and CTA^+ during alkaline treatment of USY. CTA^+ results in the formation of ordered mesoporous materials (OMMs) that are more amorphous, which can compromise the zeolite's structural integrity, and the reduction of micropore volume and weakened zeolitic characteristics, leading to lower catalytic activity compared to conventional USY. In contrast, when using TPA^+, the authors noticed that the catalyst maintains its original crystallinity without framework reorganization, leading to the formation of highly crystalline hierarchical zeolites and superior catalytic performance in the alkylation of toluene. Additionally, Gamba and Villa [88] showed that incorporating cetyltrimethylammonium bromide (CTAB) as a surfactant during desilication affects relative crystallinity and textural properties more than treatment time.

Dashtpeyma et al. [79] desilicated NaY zeolite for use as an adsorbent to remove sulfur compounds from gasoline. It was desilicated with 0.2-0.4 M NaOH or NaOH/TPAOH (65 °C, 30 min),

 doi:10.20944/preprints202512.2606.v1

then washed, dried, and calcined to yield ATY-XR samples, where X represents the TPAOH/(NaOH+TPAOH) molar ratio. Then, Metal loading was done by impregnating 5 wt.% Cu and/or Ce, followed by drying and calcination, producing CuNaY, Ce-0.5R, Cu-0.5R, and CuCe-0.5R. the results showed that among desilicated samples, ATY (0.2 M)-0.5R showed the best performance with capacities of 13.5 mg S/g (thiophene) and 15.45 mg S/g (dibenzothiophene). Metal impregnation further improved performance, with CuCe-0.5R reaching 21.02 mg S/g (thiophene) and 24 mg S/g (dibenzothiophene), attributed to the formation of additional mesopores while preserving the original micropores in the NaY zeolite. While these results demonstrate the potential of desilicated zeolite for adsorption purposes, research has more commonly focused on its catalytic applications. Jiao et al. [89] found that adding mesopores to NaY zeolite with a bulky Si/Al ratio of 5.34 by a series of treatments using lactic acid (HLA) and (NaOH or $NH_3 \cdot H_2O$) containing CTAB led to a notable enhancement in its performance during acetalization reactions such as acetalization of cyclohexanone with glycol and pentaerythritol. However, the catalyst desilicated with NaOH performed better than that with NH_3, providing conversions of (72.6 Vs 71.8) with glycol and (35.0 Vs 33.5) with pentaerythritol for a 2 h reaction time. Additionally, Gackowski et al. [90,91] emphasized the creation of extremely acidic hydroxyl groups (characterized by an IR band at 3600 cm^{-1}) when desilicating dealuminated Y zeolite (Si/Al=31) with a mixture of NaOH and tetrabutylammonium hydroxide (TBAOH), which is believed to occur during the calcination of desilicated zeolite Y in the presence of atmospheric water, which facilitates the extraction of aluminum from the framework. Also, the authors supposed that the location of these OH groups is inside supercages and can work as active sites when catalyzing reactions, like isomerization processes. These observations highlight the significance of the interplay between desilication and dealumination to create hierarchical structures that offer improved transport features, which are notably advantageous for complex reactions and reactions that include larger molecules.

2.3. Ion Exchange

Ion exchange is another significant technique in modifying zeolite Y. It refers to the substitution of the inherent cations (such as Na^+ or H^+) within the zeolite's framework with other cations. This substitution is typically achieved through either liquid-phase ion exchange (LPIE) (Figure 9) or solid-state ion exchange (SSIE) methods [92,93]. The major factors that dictate it are (1) the properties of the cation species, their sizes, hydration settings, and the charge they carry, (2) the cation species' concentrations in the solutions, (3) the anion species that coexist with the cation in those solutions, (4) solvents (the remaining water in non-aqueous solvents is essential for driving the ion-exchange process), (5) the pH readings of exchange solutions arising from cation hydrolysis, (6) the temperature at which the ion-exchange takes place, (7) the duration of the ion-exchange, (8) the three-dimensional structural shapes of frameworks, and (9) the structures' Si/Al ratios [94]. Moreover, introducing protons (H^+) into the zeolite framework is one of the common methods of ion exchange that significantly enhances the acidity of zeolite Y. The conversion from NaY to HY is typically achieved through ion exchange with ammonium (NH_4) using a strong acid solution such as NH_4NO_3 and NH_4CL, NH_4-Y zeolite is then heated at high temperatures (typically above 500 °C) to decompose the ammonium ions, releasing NH_3 and leaving behind hydrogen ions (H^+) in the zeolite framework. This process increases the number of Bronsted acid sites, which improves the zeolite's performance in various catalytic processes, including hydro-isomerization and hydrocracking [93,95–98].

 doi:10.20944/preprints202512.2606.v1

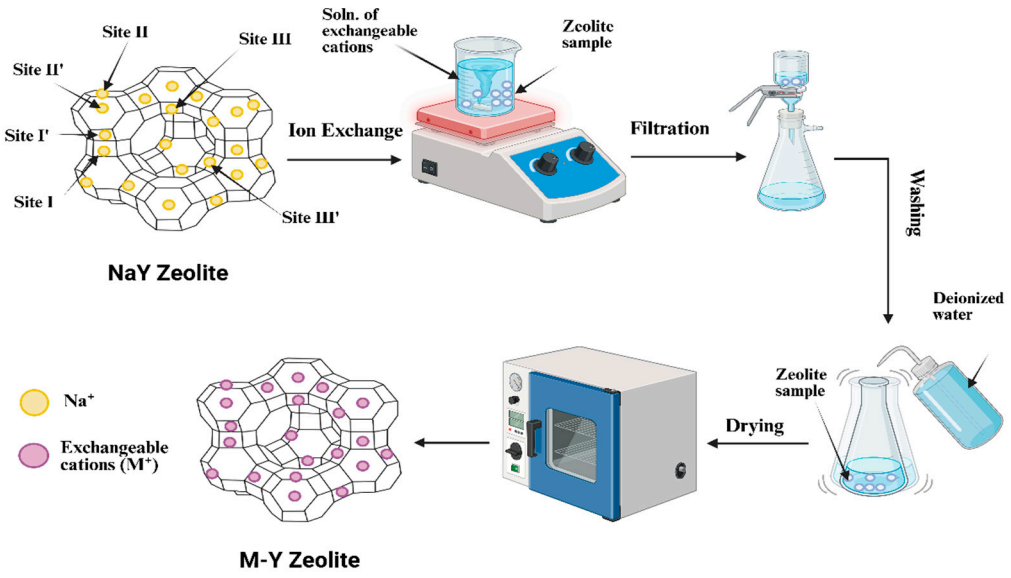

Figure 9. Schematic illustration of the ion exchange process of NaY zeolite (own elaboration based on Khalaf et al. [98] and Seo et al. [99]).

The exchange of alkali and alkaline earth metal ions is another common method employed in modifying zeolite Y. For instance, Shrestha and Dutta [100] conducted ion exchange with manganese (Mn^{2+}) and the alkaline earth metal cation (M^{2+}= Br^{2+}, Sr^{2+}, Ca^{2+}, and Mg^{2+}) to facilitate the loading of MnO_x on the zeolite to form $KMnO_x$- Y(M^{2+}), a catalyst for water oxidation. The study demonstrated that the size of the alkaline earth metal cation affects the amount of Mn^{2+} that can be exchanged into the zeolite; a larger cation leads to a decrease in the amount of Mn^{2+} and a higher catalytic rate (i.e., $KMnO_x$- Y(Br^{2+}) achieved 1.67 $mmol^{-1}$ O_2 mol^{-1} Mn s^{-1}). To understand the ion selectivity of zeolite Y, Kim et al. [101] examined the selectivity for Sr^{2+} ions in a binary solution with varying concentrations of Sr^{2+} and K^+ ions. They synthesized two distinct crystals with different Sr^{2+}/K^+ ratios (1:1 and 1:100), resulting in ion exchange degrees of 74.7% for the first crystal and 45.3% for the second one. The decrease of Sr^{2+} exchange from crystals 1 to 2 indicates that ion exchange dynamics can be manipulated through solution composition. Additionally, regarding cation affinity, the work by Khabzina et al. [102] identifies the exchange of alkali metals (i.e. K^+ and Cs^+) and alkaline earth metals (i.e. Ca^{2+}, Ba^{2+}) with zeolite Y. It highlights that bivalent cations like Ba^{2+} show a more favorable exchange compared to monovalent cations, particularly at type II sites.

The ion exchange with transition and rare earth metals has also attracted extensive scholarly focus. For transition metals, the findings by Wu et al. [103] reveal that Mn^{2+} and Zn^{2+} exchanged zeolite Y are more stable than those exchanged with Co^{2+} and Cu^{2+}. Also, the analysis by Izquierdo et al. [104] found that zeolite Y that underwent Cu^{2+} ion exchange displayed better catalytic efficiency than the one exchanged with iron ion (Fe^{2+}) in the selective catalytic reduction of nitrogen oxides from fuel gas. This emphasizes that the stability and catalytic efficiency of the zeolites vary with the type of the ion in general. Likewise, in terms of rare earth metals, Wang et al. [105] examined how La^{3+} ions behave in the ion exchange process, demonstrating that these ions can substantially improve the stability and efficiency of zeolite Y in catalytic cracking reactions. This underlines the critical role of metal cations in boosting zeolite functionalities for catalytic reaction processes, which were attributed to the presence of active metal sites created through ion exchange.

In addition to their catalytic attributes, ion-exchanged zeolite Y is extensively utilized in adsorption applications. For example, Dastanian et al. [106] used nickel-loaded zeolite Y as an absorbent for the desulfurization of heavy straight-run gasoline at ambient conditions. The Ni-Y

 doi:10.20944/preprints202512.2606.v1

zeolite exhibited excellent desulfurization capabilities. Chen et al. [107] conducted research that focused on Cu^{2+}, Co^{2+}, Ni^{2+}, and Zn^{2+} ion-exchanged zeolite Y and their performance in the selective adsorption of methyl mercaptan (CH_3SH) from natural gas. They achieved improved adsorption efficiency, especially Cu-Y zeolite, which showed the largest CH_3SH breakthrough adsorption capacity. Similarly, Chen et al. [108] applied a series of ion exchanges to zeolite Y with (Na^+, Ag^+, Cu^{2+}, Zn^{2+}, Co^{2+}, and Ni^{2+}) to use them as adsorbents for the removal of carbon disulfide (CS_2) from tail gas. They found that the samples exhibited varying adsorption capacities, with the highest CS_2 breakthrough adsorption capacity being up to 44.8 mg g^{-1} for Ag-Y zeolite. Moreover, Tobarameekul et al. [109] performed ion exchange with Zn^{2+} on synthesized zeolite NaY from rice husk ash and bagasse ash for CO_2 adsorption (Figure 10). Computational and experimental tests revealed that increasing the amount of Zn loading led to higher adsorption capacity. They also demonstrated the effect of adsorption temperature on the modified adsorbent. At lower adsorption temperatures, the process is dominated by physical adsorption, which benefits from higher surface area, while increasing temperatures beyond 873.15 K significantly reduce the CO_2 adsorption capacity due to the decreased number of adsorption sites. Djeffal et al. [110] investigated the effect of ion-exchanged zeolite Y with Cu^{2+}, Ni^{2+}, Ca^{2+}, and Na^+ in the adsorption of CO_2, resulting in an enhancement in adsorption capacity in the order of $Na^+ > Ca^{2+} > Ni^{2+} > Cu^{2+}$ with 77.57 cm^3 g^{-1} being for Na -Y zeolite, making it suitable for carbon capture and storage applications. According to Pillai et al. [111], the properties of the cation play a significant role in the adsorption of nonpolar molecules, like CO_2 and CH_4, due to electrostatic forces interacting with the zeolite's ionic surface. Furthermore, the findings from the work by Silva et al. [112] showed that Y zeolite charged with chromium (Cr) after biosorption could be effectively utilized as a catalyst for the oxidation of volatile organic compounds (VOCs), namely ethyl acetate, ethanol, and toluene. This dual functionality is advantageous in sustainability-driven processes, where materials with dual capabilities can enhance efficiency and reduce operational costs.

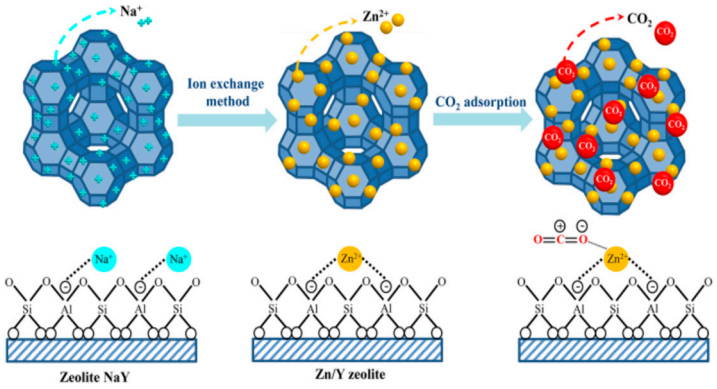

Figure 10. Schematic of the ion exchange process of NaY zeolite for CO_2 capture [109].

2.4. Surface Functionalization

One of the primary methods for modifying zeolite Y involves the incorporation of organic functional groups or nanoparticles onto its surface. Grafting is the common approaches that fall under this technique, specifically Silanation [113]. Silanation typically involves the reaction of silane compounds (often organosilanes) with hydroxyl groups on the zeolite surface, resulting in the formation of siloxane bonds (Si-O-Si). This method allows for the introduction of various functional groups that can tailor the zeolite's properties for specific purposes (Figure 11) [114]. For example, Kukwa and Dann [115] prepared 3-Aminopropyltriethoxysilane (APTES) grafted zeolite Y for the extraction of metal cations from the effluent of crude oil hydrotreatment using three different solvents (i.e., hexane, toluene and acetone). A total of 2.5 g of HY zeolite was dispersed in 40 mL of the selected solvent in a round-bottom flask and stirred under reflux conditions at 40 °C for 1 hour. Subsequently,

 doi:10.20944/preprints202512.2606.v1

6 mL of APTES was added dropwise to the suspension using a dropping pipette while maintaining continuous stirring. The reaction mixture was then refluxed at 40 °C for an additional 24 hours. Upon completion of the reaction, the APTES-functionalized zeolite Y was recovered by filtration, washed thoroughly with the same solvent and distilled water, and then dried overnight at 80 °C. The experimental analysis revealed that the optimal solvent for legend grafting was hexane. Furthermore, the selectivity tests, which evaluated the removal of Zn(II), Ni(II), V(IV), Cu(II), and Fe(II) commonly found in hydrotreatment extracts, showed substantial and fairly consistent removal efficiencies of 70.6%, 83.7%, 91.3%, 82.8%, and 85.7%, respectively.

Following the same technique, Sanaeepur et al. [116] grafted NaY zeolite with aminopropyl silanes for CO_2 separation. In their procedure, 3-aminopropyl(diethoxy)methylsilane (APDEMS) was utilized as silanization agent and has been shown to enhance CO_2 permeability in mixed matrix membranes (MMMs) by an average of 4.67%, and an increase in CO_2/N_2 selectivity of 6.34% compared to pure zeolite Y filled to MMMs. Similarly, Lu et al. [117] used N-[3-(trimethoxysilyl)propyl]ethylenediamine (AEAPTMS) as a silanizing agent. They reported that the aminosilane-functionalized zeolite Y maintained its structural integrity while enhancing its selectivity for CO_2 over CH_4 in gas separation applications. Moreover, Zhang et al. [118] compared the conventional silanization and the vapor-phase silanization overlay modification of HY zeolite. To prepare the vapor-phase grafted zeolite, 3 g of Y zeolite was placed in a quartz tube and pretreated with nitrogen at 550 °C for 2 hours, then cooled to 250 °C. A mixture of trimethylchlorosilane and nitrogen was introduced for 40 minutes, followed by a nitrogen purge to remove unreacted silane. The temperature was then raised to 550 °C, and oxygen was introduced for 1 hour to oxidize the carbonsilyl groups into a silica layer. The results showed an enhancement in the vapor-phase salinized zeolite, while maintaining nearly the same toluene adsorption performance compared to the traditional liquid-phase silanization.

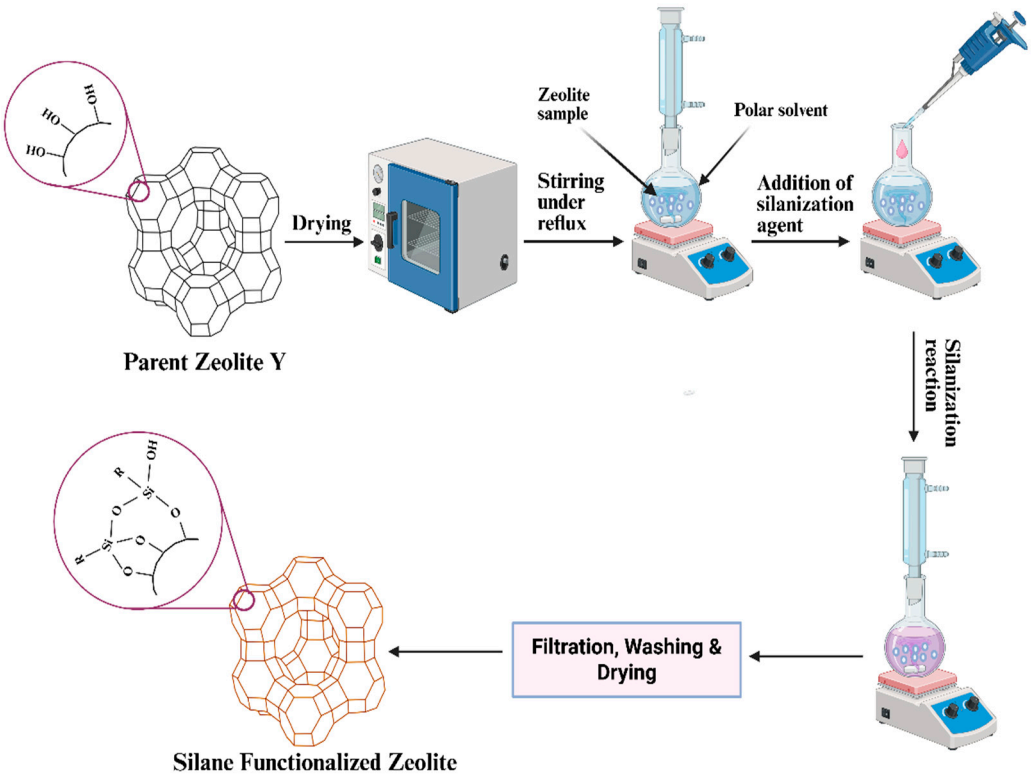

Figure 11. Schematic representation of the silanization process of Zeolite Y (own elaboration based on Kukwa and Dann [115], Sanaeepur et al. [116], Lu et al. [117]).

 doi:10.20944/preprints202512.2606.v1

Besides silane grafting, Yang et al. [119] perform small amine molecules grafting onto cobalt exchanged Y zeolite to improve CO_2 adsorption capabilities. The ion exchanged adsorbent was functionalized with ethylenediamine, achieving 4.36 mmol/g adsorption capacity, which is 1.73 times higher than unmodified zeolite. These strong interactions between the grafted amines and CO_2 molecules enhance the selectivity of the zeolite for CO_2, making it a promising candidate for carbon capture applications. Likewise, the study by Li et al. [120] focused on enhancing the separation efficiency of CH_4/N_2 using modified zeolite Y. The modification involved a two-step process: ion exchange with Zn^{2+} and grafting with the ligand 4-methylimidazole-5-carbaldehyde (almIM). The modified adsorbent, ZnY-almIM, achieved a CH_4/N_2 selectivity reaching 4.52 compared to 1.52 for pristine zeolite NaY at 298 K and 1 bar. Additionally, two-bed six-step pressure swing adsorption (PSA) simulations showed that the process could enrich a feed gas containing 50% methane to 90% methane, with a recovery rate of 87%. This proves the efficiency of modified zeolite Y in gas separation, particularly for challenging mixtures like CH_4 and N_2.

The hydrophilicity or hydrophobicity of zeolite Y can be significantly altered through surface functionalization. For instance, introducing hydrophobic functional groups by silanation, has been shown to enhance the material's hydrophobic character through the effective reduction of the free silanol groups (≡Si-OH), which are responsible for the hydrophilic nature of the zeolite. According to Wang et al. [121], hydrophobic zeolites exhibit higher adsorption rates for organic pollutants like naphthalene and chromate, despite experiencing a notable decrease in surface area and only minor crystallinity alterations. In terms of catalysis, Rahaman et al. [122] introduced n-octadecyltrichlorosilane (OTS) onto HY zeolites, resulting in a marked increase in hydrophobicity, leading to the formation of an emulsion between the two immiscible reactants, thereby minimizing the interfacial mass transfer limitation during reactions, such as glycerol acetalization with 89% conversion, whereas the unmodified HY catalyst only reached 28% conversion. Similarly, Vu et al. [123] explored the silylation of zeolite Y using different chlorosilanes. The results showed that the silyation with trichlorosilanes enhanced the hydrothermal stability of the zeolite under harsh aqueous-phase processing conditions (pH ≈ 2, T= 473 K). However, it resulted in a decrease in total specific pore volume and specific surface area. For example, the silylated zeolite Y with n-octadecyl trichlorosilane had a specific surface area of 507 m^2/g, down from 788 m^2/g for the parent zeolite Y. Also, the hydrogenation of levulinic acid to γ-valerolactone (GVL) using silylated zeolite Y showed that while stability was improved, catalytic performance was affected. Using an excess of methyltrichlorosilane improved stability but led to pore blockage, resulting in lower GVL yields (12% vs. 34% for 3PtY). These findings indicate that the introduction of hydrophobic functional groups can enhance the stability of zeolite Y in challenging environments, but it may also compromise its catalytic efficiency due to structural changes and pore blockage if not carefully managed.

Conversely, grafting with amine groups preserves their hydrophilic nature. Kim et al. [124] synthesized ethylenediamine-grafted zeolite Y via gas-phase functionalization. They have combined the strengths of both amine groups in capturing CO_2 in wet flue gas and strongly co-adsorbed H_2O within the hydrophilic Y zeolite, which helps prevent urea formation that causes the deactivation of amine-functionalized adsorbents. The resulting adsorbent demonstrated excellent regenerability, maintaining working capacities greater than 1.1 mmol g^{-1} over 20 temperature swing adsorption (TSA) cycles.

3. Impact of Post-Synthesis Modifications on Zeolite Y Properties

3.1. Structural Changes

Post-synthesis modification techniques discussed in this paper can significantly impact the structural properties of zeolite Y. Geo et al. [125] applied dealumination to two commercial zeolite Y with similar initial properties, via steaming treatment and citric acid. The modified zeolites showed an increase of the Si/Al ratio from 2.5 to 5.0 and enhanced crystallinity due to the transformation of Al from Al(IVb) to Al(V), the form of extra-framework Al species that are removed by the following citric acid treatment. However, they exhibited unequal acidic and textural characteristics due to the

 doi:10.20944/preprints202512.2606.v1

different Al migration behaviors, leading to a difference in their activity and cracking ability in the transformation of methylcyclohexane. Moreover, after the steam heating and acid treatment of granular Y zeolite, Khazipova et al. [126] found that the samples that were subjected to acid treatment only without prior steaming stabilization, experienced decationation, dealumination, and partial amorphization of its crystal lattice. In contrast, the samples that were treated with both treatments showed reduced lattice destruction. This demonstrates the importance of using both steaming and acid treatment sequentially when applying dealumination to maintain high crystallinity.

In addition, ethylenediaminetetraacetic (EDTA) treatment was found to be more effective than the hydrothermal method in increasing the Si/Al ratio and pore volume of the zeolite. The research by Moosavifar & Fathyunes [127] emphasized that as it investigated the effect of EDTA on NaY zeolite and its impact on catalyst loading. The treatment enhanced the porosity by removing extra-framework aluminum and forming secondary mesoporous structures, resulting in larger pore sizes, improved pore volume, and higher catalyst loading of molybdophosphoric acid (MPA) in the supercage of zeolite, achieving (0.049 mmol/g support) compared to (0.043 mmol/g support) with the hydrothermal method. Moreover, utilizing a microwave reactor combined with chemical treatment has recently proven highly effective in this field for its numerous advantages, including reduced reaction times, targeted and homogenous heating, lower energy consumption, and minimized environmental impact [128–130]. Abdulridha et al. [131] performed microwave-assisted chemical treatment using (H_2EDTA). The treatment significantly enhanced the intracrystalline mesoporosity of zeolite Y, achieving an external surface area of 287 m^2/g in just 1 minute compared to 205 m^2/g after 6 hours of conventional hydrothermal treatment. In another study, Abdulridha et al. [60] applied microwave-assisted chelation using EDTA to a parent zeolite Y, obtaining better results for the external surface area of >300 m^2/g and mesopore volumes of >0.46 cm^3/g.

In a different approach, Ion exchange significantly alters the porosity of zeolites as stated by the study by Zhu et al. [132]. They found that adding mono- and di-valent cations through ion exchange affects the channel structure of the NaY zeolite membranes. The study also mentions that the degree of ion exchange varies with different cations. For instance, Ag^+ and K^+ showed high cation exchange degrees (96.54% and 82.77%), leading to noticeable changes in the overall porosity of the membrane. Additionally, the work by Seo et al. [94] highlighted that the ion exchange with Ni^{2+} resulted in a slight decrease in crystallinity while maintaining the overall framework intact. This finding is important because it indicates that although ion exchange can alter the characteristics of zeolite, precise management of the procedure can minimize negative impacts on its structure.

To understand the impact of these approaches on the zeolite Y's structural properties, characterization techniques are essential. Various methods provide insights into crystallinity, framework stability, and porosity. Table 1 gives an overview of the different characterization techniques commonly employed in zeolite research, supported by relevant literature.

Table 1. The common characterization techniques used to characterize the structural properties of zeolite Y.

Characterization Technique	Purpose	Typical Conditions	Example in Literature	Ref.
XRD	Determine crystalline structure and phase purity.	Ambient; powdered samples; X-rays	XRD was used to confirm the crystalline structure of synthesized hexagonal zeolite Y from Kankara kaolin.	[133,134]
SEM	Study surface morphology and particle size.	Vacuum; conductive coating required	SEM was used to analyze the microstructure of nanocrystalline zeolite Y.	[135,136]
TEM	Provide detailed internal structure and morphology at an atomic scale.	High vacuum; ultrathin samples	The mesopores of the zeolite Y (CBV 720) containing platinum tracking were visualized by TEM, including inside crystals and those that emerge at its surface.	[137,138]
BET	Determine surface area, pore volume, and pore size distribution.	Liquid nitrogen; under vacuum, gas adsorption	The specific surface area of nano zeolite Y (NFA-Y) that was synthesized from fly ash was obtained by BET	[139,140]
NMR	Analyze local chemical environment	Ambient; solid-state or powdered	27Al NMR showed steam calcination reduces framework aluminum, creating extra-	[141,142]

 doi:10.20944/preprints202512.2606.v1

		samples; magnetic field	framework aluminum that alters the acidity and catalytic behavior of USY.	
Raman	Provide information on vibrational modes of the framework.	Ambient; laser excitation	Raman was utilized to analyze the vibrational spectra of zeolite Y after ion exchange with different cations, comparing computed spectra of optimized structures with experimental data.	[143,144]

As evidenced by the previous studies mentioned in this section, these treatments can significantly enhance Zeolite Y's crystallinity, framework stability, and porosity as they allow for tailored adjustments at atomic, micropore, and crystal levels, optimizing the material's performance for specific applications beyond the limitations of initial synthesis conditions.

3.2. Physicochemical Properties

The stability of modified Zeolite Y is often superior to that of unmodified zeolites. Vu et al. [145] improved the hydrothermal stability of zeolite Y by incorporating lanthanum (La^{3+}) cations into its framework through ion exchange and used it as a catalyst for the aqueous-phase hydrogenation of levulinic acid (LA) with formic acid (FA). They tested its stability by subjecting it to a reaction mixture (0.2 mol/ L LA, 0.6 mol/ L FA) at 473 K under autogenous pressure for 24 h. After the hydrothermal treatment, the zeolite with the highest La content (0.5 mmol/ g) demonstrates the highest stability, maintaining 25% of its original specific micropore volume, while unmodified zeolite Y entirely loses its microporosity. A pivotal element contributing to this stabilization is the preservation of the structural integrity of the zeolite framework. This preservation is realized through a multi-core rare earth bridging structure, which incorporates a greater number of non-skeletal oxygen atoms. This structure helps maintain the zeolite's framework under harsh conditions. [146,147]. Furthermore, Buttersack et al. [148] investigated the stability of highly dealuminated zeolite Y within aqueous media. The stability assessment of Y zeolite in both pure water and NaCl solution across varying pH levels revealed that the hydrothermal stability of high-silica zeolite is comparatively higher, but the presence of Na^+ ions significantly accelerates the degradation of the zeolite structure.

Altering the Bronsted and Lewis acid sites of zeolite Y through dealumination and desilication processes markedly impacts their catalytic properties. Dealumination leads to the generation of tri-coordinated aluminum, which acts as a Lewis acid site, crucial for catalytic reactions like oxidative desulfurization [149]. Wang et al. [150] achieved an increase in the Si/Al ratio of 2.7 after a mild steam treatment of a parent zeolite Y. They noted that the concentration of Bronsted acid sites decreases with dealumination, but the remaining sites exhibit increased strength due to a reduced framework aluminum content. Additionally, Li et al. [151] investigate the spatial proximities among acid sites in dealuminated H-Y zeolites. As a result, the extra framework AlOH species (Lewis acid sites) are consistently located near bridging AlOHSi hydroxyls (Bronsted acid sites) in zeolites treated by thermal and hydrothermal methods, creating a synergistic effect that improves the catalytic activity. On the other hand, during desilication, aluminum is reinserted into the zeolite framework, forming tetrahedral coordination similar to amorphous aluminosilicates, which can generate both Bronsted and Lewis acid sites [91].

All the above changes in chemical and physical properties cannot be evaluated if it were not for characterization techniques, which are listed in Table 2.

Table 2. The common characterization techniques used to characterize the physicochemical properties of zeolite Y.

Characterization Technique	Purpose	Typical Conditions	Example in Literature	Ref.
FTIR	Identify functional groups and framework vibrations.	Ambient; powdered or pellet samples	FTIR confirmed the successful synthesis of zeolite NaY from Rice husk ash by identifying the distinct functional groups, such as Si-O and Al-O stretches.	[152,153]

 doi:10.20944/preprints202512.2606.v1

XRF	Determine elemental composition.	Ambient; solid or powdered samples	XRF measured the elemental content in zeolite Y synthesized from natural clay.	[154]
TGA	Study thermal stability and decomposition behavior.	commonly up to 1000°C, controlled atmosphere (air or inert)	The thermal stability of NaTMA-Y zeolite was quantified before and after activation utilizing TGA, which revealed a mass loss between (625-1050K) due to the decomposition of the TMA^+ cations.	[155,156]
NH_3-TPD	Determines the acidity strength and distribution of acidic sites.	Variable temperatures; controlled ammonia gas flow	NH_3-TPD analysis showed that modified zeolite Y via dealumination increased the concentration of strong acid sites.	[157]
EPR	Study paramagnetic species and defects.	Ambient or low temperatures; under magnetic field	EPR identified the formation of Cu^{2+} NO_3^- species at room temperature in Cu-Y zeolites when used for the catalytic reduction of NO_x with hydrocarbons.	[158,159]
ICP-OES	determining the elemental composition and metal loading	Ambient; sample digested in solution	The Si/Al ratio of modified zeolite Y with iron species was measured using ICP-OES.	[160,161]
DR UV-Vis	Analyze electronic transitions in metal-substituted zeolites.	Ambient; solid samples in diffuse reflectance mode	DR UV-Vis is used to study the electronic transitions in the FeY zeolite, helping to identify the presence and nature of iron species within the zeolite structure.	[162]

Moreover, the performance of modified Zeolite Y in specific reactions, such as the transesterification of waste cooking oil for biodiesel production, has demonstrated that modifications can lead to significant improvements in conversion rates and product yields compared to unmodified zeolite [163]. This is indicative of the broader applicability of modified zeolites across various catalytic processes, where the tuning of physicochemical properties can lead to optimized performance.

4. Limitations and Future Prospects

Although post-synthesis modification has significantly enhanced its applicability, several constraints continue to influence the extent to which these techniques can be executed. One of the main challenges is maintaining the stability of the FAU framework during treatments such as dealumination and desilication. Too aggressive dealumination might lead to structural disintegration, loss of crystalline structure, and the appearance of unwanted non-framework species, all significantly impacting the acidity and molecular diffusion of zeolite. Desilication presents similar challenges as alkaline solutions can easily over-etch the framework, resulting in inconsistent mesoporosity and sometimes destroying micropores. Consequently, creating uniform and predictable pore structures remains difficult. Moreover, the uneven distribution of active sites after modifications like ion exchange, metal loading, or steaming is another issue. Incomplete exchanges, or the formation of EFAL can produce catalysts with performance variations that exceed anticipated levels. Scaling up these processes is also not straightforward. Many post-treatment procedures, particularly those that necessitate careful leaching, multi-stage exchanges, or template-based methods, are hard to reproduce consistently on a large scale, and they increase production costs. Environmental concerns add further complications. Acidic, alkaline, and solvent-intensive processes generate waste that must be properly managed, which may reduce the appeal of these methods for industrial applications. Even after successful modifications, researchers frequently face a trade-off; enhancing molecular transport through the creation of mesopores comes at the cost of the density of strong Bronsted acid sites, thereby potentially compromising catalytic efficacy for reactions reliant on acidity. Despite these challenges, several promising avenues could steer future advancements. More refined and mild modification pathways, such as the utilization of chelating agents, may facilitate precise control over the Si/Al ratio without compromising the integrity of the framework. New strategies for generating hierarchical pores without surfactants or excessive chemical usage, including dry-gel or steam-assisted approaches, could make the process more sustainable and reproducible. Improvements in characterization techniques, such as in-situ NMR and high-resolution microscopy, will also give clearer insights into the structural evolution during treatment, helping

 doi:10.20944/preprints202512.2606.v1

researchers design modifications more deliberately. Another area with considerable potential is the incorporation of single-atom metals or dual-function sites. If metals can be anchored more firmly within the FAU structure, Zeolite Y could be customized for reactions in fuel upgrading, alkylation, or biomass conversion with much higher precision. Computational tools and machine-learning-based screening may also help identify optimal treatment conditions more efficiently. Finally, the development of greener and more scalable methodologies that employ reduced solvent usage, lower energy inputs, or alternative activation techniques will be essential for the long-term industrial integration of these processes. Moving ahead, research is likely to concentrate on formulating modification strategies that strike a balance between pore architecture, acidity, and stability for specific catalytic or adsorption applications. Overcoming these challenges through careful engineering and sustainable practices will play a key role in advancing the next generation of high-performance Zeolite Y materials.

5. Conclusions

The post-synthesis modification techniques discussed herein underscore the significance of customized treatments in enhancing the performance of zeolite Y. Dealumination methods, whether conducted via acidic, steaming, or chemical means and augmented by innovative strategies such as ultrasound, proficiently enhance the Si/Al ratio while generating more robust and accessible acid sites. Desilication, through alkaline treatments, generates mesoporosity and enhances mass transport as well, especially when combined with dealumination. Ion exchange further enriches the functional potential of zeolite Y by fine-tuning its cationic composition, consequently modifying both its acidity and adsorption properties. Meanwhile, Surface functionalization through silanation and grafting not only alters the hydrophilic/hydrophobic balance but also amplifies the selectivity for specific applications. Advanced modification approaches, including microwave-assisted processing, manifest as promising and energy-efficient alternatives to traditional methods. These strategies enable the development of multifunctional zeolite Y materials with superior catalytic, adsorption, and separation properties. Future research should focus on integrating these methodologies alongside the optimization of process parameters to prepare zeolite Y for emerging applications like CO_2 capture, biofuel production, and green chemistry transformations, thus ensuring its ongoing relevance in sustainable industrial processes.

Author Contributions: Conceptualization, A.A., W.A.-M. and A.B.J.; methodology, W.A.-M. and A.B.J.; formal analysis, W.A.-M.; investigation, A.A. and A.M.; writing—original draft preparation, A.A.; writing—review and editing, S.H., A.M. and A.B.J.; visualization, A.A. and S.H.; validation, S.H. and A.M.; supervision, W.A.-M. and A.B.J. All authors have read and agreed to the published version of the manuscript.

Funding: This research received no external funding.

Data Availability Statement: No new data were created or analyzed during this study. Data sharing is not applicable to this article.

Conflicts of Interest: The authors declare no conflicts of interest.

Abbreviations

The following abbreviations are used in this manuscript:

FAU	Faujasite framework
USY	Ultra-Stable Y Zeolite
EFAl	Extra-Framework aluminum
AFS	Ammonium fluosilicate
EDTA	Ethylene diamine tetraacetic acid
AHFS	Ammonium hexafluorosilicate
NaOH	Sodium hydroxide
TAAOH	Tetraalkylammonium hydroxide

 doi:10.20944/preprints202512.2606.v1

TPA	Tetrapropylammonium
CTA	Cetyltrimethylammonium
OMM	Ordered mesoporous material
CTAB	Cetyltrimethylammonium bromide
TPAOH	Tetrapropylammonium hydroxide
TBAOH	Tetrabutylammonium hydroxide
LPIE	Liquid-phase ion exchange
SSIE	Solid-state ion exchange
VOC	Volatile organic compound
APTES	3-Aminopropyltriethoxysilane
APDEMS	3-aminopropyl(diethoxy)methylsilane
MMM	Mixed matrix membrane
AEAPTMS	N-[3-(trimethoxysilyl)propyl]ethylenediamine ()
PSA	Pressure swing adsorption
OTS	N-octadecyltrichlorosilane
TSA	Temperature swing adsorption
XRD	X-ray diffraction
SEM	Scanning electron microscopy
TEM	Transmission electron microscopy
BET	Brunauer–Emmett–Teller surface area analysis
NMR	Nuclear magnetic resonance spectroscopy
Raman	Raman spectroscopy
FTIR	Fourier transform infrared spectroscopy
XRF	X-ray fluorescence spectroscopy
TGA	Thermogravimetric analysis
NH_3-TPD	Ammonia temperature-programmed desorption
EPR	Electron paramagnetic resonance spectroscopy

References

1. A. F. Cronstedt, Rön och beskrifning om en obekant bärg art, som kallas Zeolites. 1756.
2. M. A. Damour, “Sur quelques minéraux connus sous le nom de quartz résinite,” Ann. Mines, vol. 3, pp. 191–202, 1840.
3. H. Eichhorn, “Ueber die einwirkung verdünnter salzlösungen auf silicate,” Ann Phys, vol. 181, no. 9, pp. 126–133, 1858.
4. H. de S. Claire-Deville, “Reproduction de la levyne,” Comptes Rendus, vol. 54, no. 1862, pp. 324–327, 1862.
5. G. Friedel, “Sur quelques proprietés nouvelles des zéolithes,” Bulletin de Minéralogie, vol. 19, no. 3, pp. 94–118, 1896.
6. M. F. Grandjean, “Étude optique de l’absorption des vapeurs lourdes par certaines zéolithes,” CR Acad. Sci, vol. 149, pp. 866–868, 1909.
7. O. Weigel and E. Steinhoff, “IX. Die Aufnahme organischer Flüssigkeitsdämpfe durch Chabasit,” Zeitschrift für Kristallographie-Crystalline Materials, vol. 61, no. 1–6, pp. 125–154, 1924.
8. L. Pauling, “The structure of some sodium and calcium aluminosilicates,” Proceedings of the National Academy of Sciences, vol. 16, no. 7, pp. 453–459, 1930.
9. L. Pauling, “XXII. The Structure of Sodalite and Helvite.,” Zeitschrift für Kristallographie-Crystalline Materials, vol. 74, no. 1–6, pp. 213–225, 1930.
10. W. H. Taylor, “I. The structure of analcite (NaAlSi2O6· H2O,” Zeitschrift für Kristallographie-Crystalline Materials, vol. 74, no. 1–6, pp. 1–19, 1930.
11. J. W. McBain, “The Sorption of Gases and Vapours by Solids.,” J Phys Chem, vol. 37, no. 1, pp. 149–150, 2002.
12. R. M. Barrer, “The sorption of polar and non-polar gases by zeolites,” Proc R Soc Lond A Math Phys Sci, vol. 167, no. 930, pp. 392–420, 1938.
13. R. M. Barrer, “Migration in crystal lattices,” Transactions of the Faraday Society, vol. 37, pp. 590–599, 1941.
14. R. M. Barrer and E. A. D. White, “286. The hydrothermal chemistry of silicates. Part II. Synthetic crystalline sodium aluminosilicates,” Journal of the Chemical Society (Resumed), pp. 1561–1571, 1952.

 doi:10.20944/preprints202512.2606.v1

15. R. M. Barrer and D. W. Riley, "34. Sorptive and molecular-sieve properties of a new zeolitic mineral," Journal of the Chemical Society (Resumed), pp. 133–143, 1948.
16. R. M. Barrer, "33. Synthesis of a zeolitic mineral with chabazite-like sorptive properties," Journal of the Chemical Society (Resumed), pp. 127–132, 1948.
17. R. M. Barrer and D. J. Robinson, "The structures of the salt-bearing aluminosilicates, Species P and Q," Zeitschrift für Kristallographie, vol. 135, no. 5–6, pp. 374–390, 1972.
18. R. M. Barrer, "Preparation of some crystalline hydrogen zeolites," Nature, vol. 164, no. 4159, pp. 112–113, 1949.
19. R. M. Barrer and P. J. Denny, "201. Hydrothermal chemistry of the silicates. Part IX. Nitrogenous aluminosilicates," Journal of the Chemical Society (Resumed), pp. 971–982, 1961.
20. R. M. Barrer, P. J. Denny, and E. M. Flanigen, "Molecular sieve adsorbents," Feb. 28, 1967, Google Patents.
21. R. M. Barrer and H. Villiger, "Probable structure of zeolite Ω," Journal of the Chemical Society D: Chemical Communications, no. 12, pp. 659–660, 1969.
22. C. Martínez and J. Pérez-Pariente, "Zeolites and ordered porous solids: fundamentals and applications," Valencia, Spain: FEZA, 2011.
23. S. I. Zones, "Translating new materials discoveries in zeolite research to commercial manufacture," Microporous and Mesoporous materials, vol. 144, no. 1–3, pp. 1–8, 2011.
24. L. Gómez-Hortigüela and B. Bernardo-Maestro, Insights into the chemistry of organic structure-directing agents in the synthesis of zeolitic materials. Springer, 2018.
25. R. M. Milton, "Molecular Sieve Science and Technology," pp. 1–10, Jul. 1989, doi: 10.1021/BK-1989-0398.CH001.
26. E. M. Flanigen and J. A. Rabo, "A tribute to Robert Mitchell Milton, zeolite pioneer (1920-2000)-Obituary," 2001, ELSEVIER SCIENCE BV PO BOX 211, 1000 AE AMSTERDAM, NETHERLANDS.
27. R. M. Milton, "Molecular sieve adsorbents," Apr. 14, 1959, Google Patents.
28. D. W. Breck, W. G. Eversole, R. M. Milton, T. B. Reed, and T. L. Thomas, "Crystalline zeolites. I. The properties of a new synthetic zeolite, type A," J Am Chem Soc, vol. 78, no. 23, pp. 5963–5972, 1956.
29. D. W. Breck, W. G. Eversole, and R. M. Milton, "New synthetic crystalline zeolites," J Am Chem Soc, vol. 78, no. 10, pp. 2338–2339, 1956.
30. T. B. Reed and D. W. Breck, "Crystalline zeolites. II. Crystal structure of synthetic zeolite, type A," J Am Chem Soc, vol. 78, no. 23, pp. 5972–5977, 1956.
31. E. M. Flanigen, J. C. Jansen, and H. van Bekkum, Introduction to zeolite science and practice. Elsevier, 1991.
32. E. M. Flanigen, R. W. Broach, and S. T. Wilson, "Zeolites in industrial separations and catalysis. Zeolites in Industrial Separation and Catalysis. 1–26," 2010.
33. V. Verdoliva, M. Saviano, and S. De Luca, "Zeolites as acid/basic solid catalysts: recent synthetic developments," Catalysts, vol. 9, no. 3, p. 248, 2019.
34. H. Pines, The chemistry of catalytic hydrocarbon conversions. Elsevier, 2012.
35. J. Weitkamp, "Zeolites and catalysis," Solid State Ion, vol. 131, no. 1–2, pp. 175–188, 2000.
36. A. Primo and H. Garcia, "Zeolites as catalysts in oil refining," Chem Soc Rev, vol. 43, no. 22, pp. 7548–7561, 2014.
37. L. B. McCusker and C. Baerlocher, "Zeolite structures," in Studies in Surface Science and Catalysis, vol. 157, Elsevier, 2005, pp. 41–64.
38. C. H. Bartholomew and R. J. Farrauto, Fundamentals of industrial catalytic processes. John Wiley & Sons, 2011.
39. Kamlesh Sahu, "STUDIES ON THE SYNTHESIS AND CHARACTERIZATION OF ZEOLITES AND THEIR APPLICATION AS A CATALYST," International Journal for Research Publication and Seminar, vol. 15, pp. 357–364, Sep. 2024, doi: 10.36676/jrps.v15.i3.1518.
40. S. Qiu et al., "Zeolite-Based Materials for Catalytic Oxidation of Volatile Organic Compounds," 2024, John Wiley and Sons Inc. doi: 10.1002/cctc.202401443.
41. Q. Lang, P. Lu, X. Yang, and V. Valtchev, "Zeolites for the environment," Green Carbon, vol. 2, pp. 12–32, Mar. 2024, doi: 10.1016/j.greenca.2024.02.007.

 doi:10.20944/preprints202512.2606.v1

42. W. Zhang et al., "Recent Progress on the Synthesis and Applications of Zeolites from Industrial Solid Wastes," Catalysts, vol. 14, p. 734, Oct. 2024, doi: 10.3390/catal14100734.
43. M. A. den Hollander, M. Wissink, M. Makkee, and J. A. Moulijn, "Gasoline conversion: reactivity towards cracking with equilibrated FCC and ZSM-5 catalysts," Appl Catal A Gen, vol. 223, no. 1–2, pp. 85–102, 2002.
44. K. Sun, J. Lu, L. Ma, Y. Han, Z. Fu, and J. Ding, "A comparative study on the catalytic performance of different types of zeolites for biodiesel production," Fuel, vol. 158, pp. 848–854, 2015.
45. P. K. Bajpai, "Synthesis of mordenite type zeolite," Zeolites, vol. 6, no. 1, pp. 2–8, 1986.
46. V. Komvokis, L. X. L. Tan, M. Clough, S. S. Pan, and B. Yilmaz, "Zeolites in fluid catalytic cracking (FCC)," Zeolites in Sustainable Chemistry: Synthesis, Characterization and Catalytic Applications, pp. 271–297, 2016.
47. W. Li, J. Zheng, Y. Luo, C. Tu, Y. Zhang, and Z. Da, "Hierarchical Zeolite Y with Full Crystallinity: Formation Mechanism and Catalytic Cracking Performance," Energy and Fuels, vol. 31, pp. 3804–3811, Apr. 2017, doi: 10.1021/acs.energyfuels.6b03421.
48. R. Simancas et al., "Recent progress in the improvement of hydrothermal stability of zeolites," Jun. 2021, Royal Society of Chemistry. doi: 10.1039/d1sc01179k.
49. J. Zang, H. Yu, G. Liu, M. Hong, J. Liu, and T. Chen, "Research Progress on Modifications of Zeolite Y for Improved Catalytic Properties," Jan. 2023, MDPI. doi: 10.3390/inorganics11010022.
50. Y. D. G. Edañol, K. A. S. Usman, S. Jr. C. Buenviaje, M. E. Mantua, and L. Jr. M. Payawan, "Utilizing Silica from Rice Hull for the Hydrothermal Synthesis of Zeolite Y," KIMIKA, vol. 29, pp. 17–21, Jun. 2018, doi: 10.26534/kimika.v29i1.17-21.
51. S. Jafari, H. Asilian Mahabady, and H. Kazemian, "Gold-nano particles supported on Na-Y and H-Y types zeolites: Activity and thermal stability for CO oxidation reaction," Catal Letters, vol. 128, pp. 57–63, Mar. 2009, doi: 10.1007/s10562-008-9724-x.
52. B. Meng et al., "Synthesis of USY zeolite with a high mesoporous content by introducing Sn and enhanced catalytic performance," Ind Eng Chem Res, vol. 59, no. 13, pp. 5712–5719, 2020.
53. J. Scherzer and A. P. Humphries, "Dealumination of faujasite-type zeolites using ion exchange resins," Apr. 23, 1985, Google Patents.
54. T. Yoshioka, K. Iyoki, Y. Yanaba, T. Okubo, and T. Wakihara, "Dealumination of RHO zeolite by acid treatment and recrystallization with organic pore filler," Journal of the Ceramic Society of Japan, vol. 132, no. 2, pp. 45–49, 2024.
55. P. Huifang, W. Xiaofeng, Z. Yewen, and S. Zhihong, "The dealumination process of acid attack and coking behaviour in ultrastable Y zeolites," in Studies in Surface Science and Catalysis, vol. 88, Elsevier, 1994, pp. 223–231.
56. L. Buchori and D. D. Anggoro, "Modification of zeolite Y as a catalyst in the production of dimethyl ether from methanol dehydration," Journal of Engineering Research, 2022.
57. A. Maghfirah, Y. Susanti, A. T. N. Fajar, R. R. Mukti, and G. T. M. Kadja, "The role of tetraalkylammonium for controlling dealumination of zeolite y in acid media," Mater Res Express, vol. 6, Jun. 2019, doi: 10.1088/2053-1591/ab0eff.
58. M.-C. Silaghi, "Ab initio molecular modelling of the dealumination and desilication mechanisms of relevant zeolite frameworks," 2014.
59. Y. Kamimura, T. Kodaira, H. Yamada, N. Hiyoshi, and A. Endo, "Direct Visualization of the Dealumination Process on Zeolite Y: How Was the Mesoporous Architecture Formed?," Chemistry of Materials, vol. 37, no. 8, pp. 2735–2748, Apr. 2025, doi: 10.1021/ACS.CHEMMATER.4C03233.
60. S. Abdulridha et al., "An efficient microwave-assisted chelation (MWAC) post-synthetic modification method to produce hierarchical Y zeolites," Microporous and Mesoporous Materials, vol. 311, p. 110715, 2021.
61. W. Lutz et al., "Investigations of the mechanism of dealumination of zeolite Y by steam: Tuned mesopore formation versus the Si/Al ratio," in Studies in Surface Science and Catalysis, Elsevier Inc., 2004, pp. 1411–1417. doi: 10.1016/s0167-2991(04)80658-x.
62. W. Lutz, "Zeolite Y: Synthesis, modification, and properties—A case revisited," Advances in Materials Science and Engineering, vol. 2014, no. 1, p. 724248, 2014.

 doi:10.20944/preprints202512.2606.v1

63. O. Pliekhov et al., "Study of water adsorption on EDTA dealuminated zeolite Y," Microporous and Mesoporous Materials, vol. 302, Aug. 2020, doi: 10.1016/j.micromeso.2020.110208.
64. J. Pérez-Ramírez, C. H. Christensen, K. Egeblad, C. H. Christensen, and J. C. Groen, "Hierarchical zeolites: enhanced utilisation of microporous crystals in catalysis by advances in materials design," Chem Soc Rev, vol. 37, no. 11, pp. 2530–2542, 2008.
65. C. Manrique, R. Solano, C. Mendoza, S. Amaya, and A. Echavarría, "Hierarchical submicrosized Y zeolites prepared by sequential desilication–dealumination post-synthesis modification and their catalytic performance in vacuum gas oil hydrocracking," New Journal of Chemistry, vol. 48, no. 14, pp. 6188–6200, 2024.
66. K. Qiao et al., "An efficient modification of ultra-stable Y zeolites using citric acid and ammonium fluosilicate," Appl Petrochem Res, vol. 4, pp. 373–378, 2014.
67. X. Li et al., "Combined modification of ultra-stable Y zeolites via citric acid and phosphoric acid," Appl Petrochem Res, vol. 4, pp. 343–349, 2014.
68. K. Qiao et al., "Modification of USY zeolites with malic–nitric acid for hydrocracking," Appl Petrochem Res, vol. 6, pp. 353–359, 2016.
69. K. Qiao, L. Wei, R. Feng, Z. Yan, Z. Zhang, and X. Gao, "Preparation and characterization of hierarchical USY by post-treatment," Appl Petrochem Res, vol. 5, pp. 313–319, 2015.
70. M. Hosseini, M. A. Zanjanchi, B. Ghalami-Choobar, and H. Golmojdeh, "Ultrasound-assisted dealumination of zeolite y," Journal of Chemical Sciences, vol. 127, pp. 25–31, 2015, doi: 10.1007/s12039-014-0745-2.
71. S. Esmaeili, M. A. Zanjanchi, H. Golmojdeh, and F. Mizani, "Increasing the adsorption capabilitiy of mordenite and Y zeolites via post-synthesis chemical/physical treatments in order to remove cationic dyes from polluted water," Water and Environment Journal, vol. 34, pp. 117–130, Feb. 2020, doi: 10.1111/wej.12446.
72. C. S. Triantafillidis and N. P. Evmiridis, "Dealuminated H− Y zeolites: influence of the number and type of acid sites on the catalytic activity for isopropanol dehydration," Ind Eng Chem Res, vol. 39, no. 9, pp. 3233–3240, 2000.
73. G. Agostini et al., "In situ XAS and XRPD parametric rietveld refinement to understand dealumination of Y zeolite catalyst," J Am Chem Soc, vol. 132, pp. 667–678, Jan. 2010, doi: 10.1021/ja907696h.
74. K. S. Yoo, S. Gopal, and P. G. Smirniotis, "Enhancement of n-hexane cracking activity over modified ZSM-12 zeolites," Ind Eng Chem Res, vol. 44, no. 13, pp. 4562–4568, 2005.
75. A. V. Yakimov et al., "Dealumination of Nanosized Zeolites Y," Petroleum Chemistry, vol. 59, pp. 540–545, May 2019, doi: 10.1134/S0965544119050116.
76. D. Verboekend, M. Milina, S. Mitchell, and J. Pérez-Ramírez, "Hierarchical zeolites by desilication: Occurrence and catalytic impact of recrystallization and restructuring," Cryst Growth Des, vol. 13, no. 11, pp. 5025–5035, 2013.
77. D. Liang, Y. Liu, R. Zhang, Q. Xie, and L. Zhang, "A Review on the Influence Factors in the Synthesis of Zeolites and the Transformation Behavior of Silicon and Aluminum During the Process," 2024, Taylor and Francis Ltd. doi: 10.1080/02603594.2024.2309878.
78. J. R. García, M. Falco, and U. Sedran, "Impact of the Desilication Treatment of y Zeolite on the Catalytic Cracking of Bulky Hydrocarbon Molecules," Top Catal, vol. 59, pp. 268–277, Feb. 2016, doi: 10.1007/s11244-015-0432-7.
79. G. Dashtpeyma, S. R. Shabanian, J. Ahmadpour, and M. Nikzad, "Effect of desilication of NaY zeolite on sulfur content reduction of gasoline model in presence of toluene and cyclohexene," Chemical Engineering Research and Design, vol. 178, pp. 523–539, Feb. 2022, doi: 10.1016/J.CHERD.2021.12.041.
80. Y. Han, K. Larmier, M. Rivallan, and G. D. Pirngruber, "Generation of mesoporosity in H–Y zeolites by basic or acid/basic treatments: Towards a guideline of optimal Si/Al ratio and basic reagent," Microporous and Mesoporous Materials, vol. 365, Feb. 2024, doi: 10.1016/j.micromeso.2023.112906.
81. D. Verboekend, T. C. Keller, S. Mitchell, and J. Pérez-Ramírez, "Hierarchical FAU-and LTA-type zeolites by post-synthetic design: a new generation of highly efficient base catalysts," Adv Funct Mater, vol. 23, no. 15, pp. 1923–1934, 2013.

 doi:10.20944/preprints202512.2606.v1

82. R. Zhang et al., "Using ultrasound to improve the sequential post-synthesis modification method for making mesoporous Y zeolites," Front Chem Sci Eng, vol. 14, pp. 275–287, 2020.
83. C. Pagis, A. R. M. Prates, N. Bats, A. Tuel, and D. Farrusseng, "High-silica hollow Y zeolite by selective desilication of dealuminated NaY crystals in the presence of protective Al species," CrystEngComm, vol. 20, no. 11, pp. 1564–1572, 2018.
84. J. Mandela, W. Trisunaryanti, T. Triyono, M. Koketsu, and D. A. Fatmawati, "Hydrochloric Acid and/or Sodium Hydroxide-modified Zeolite Y for Catalytic Hydrotreating of α-Cellulose Bio-Oil," Indonesian Journal of Chemistry, vol. 21, no. 4, pp. 787–796.
85. D. Verboekend, G. Vilé, and J. Pérez-Ramírez, "Mesopore formation in usy and beta zeolites by base leaching: Selection criteria and optimization of pore-directing agents," Cryst Growth Des, vol. 12, pp. 3123–3132, Jun. 2012, doi: 10.1021/cg3003228.
86. D. Verboekend and J. Pérez-Ramírez, "Desilication mechanism revisited: Highly mesoporous all-silica zeolites enabled through pore-directing agents," Chemistry - A European Journal, vol. 17, pp. 1137–1147, Jan. 2011, doi: 10.1002/chem.201002589.
87. D. Verboekend, G. Vilé, and J. Pérez-Ramírez, "Hierarchical Y and USY zeolites designed by post-synthetic strategies," Adv Funct Mater, vol. 22, no. 5, pp. 916–928, 2012.
88. C. F. Imbachi-Gamba, J. P. Cano-Restrepo, and A. L. Villa, "Effect of the Desilication Conditions on the Synthesis of Hierarchical Zeolite Y," in 2019 North American Catalysis Society Meeting, NAM, 2019.
89. W. Q. Jiao, W. H. Fu, X. M. Liang, Y. M. Wang, and M. Y. He, "Preparation of hierarchically structured y zeolite with low Si/Al ratio and its applications in acetalization reactions," RSC Adv, vol. 4, pp. 58596–58607, Oct. 2014, doi: 10.1039/c4ra11042k.
90. M. Gackowski, Ł. Kuterasiński, J. Podobiński, and J. Datka, "Hydroxyl groups of exceptionally high acidity in desilicated zeolites Y," ChemPhysChem, vol. 19, no. 24, pp. 3372–3379, 2018.
91. M. Gackowski, J. Podobiński, E. Broclawik, and J. Datka, "IR and NMR Studies of the status of Al and acid sites in desilicated zeolite Y," Molecules, vol. 25, no. 1, p. 31, 2019.
92. M. Zendehdel, M. Kooti, and M. M. Amini, "Dispersion and solid state ion exchange of VCl3, CrCl 3·6H2O, MnCl2·4H2O and CoCl2·6H2O onto the surface of NaY zeolite using microwave irradiation," Journal of Porous Materials, vol. 12, pp. 143–149, Apr. 2005, doi: 10.1007/s10934-005-6771-1.
93. T. Alam, Y. K. Krisnandi, W. Wibowo, D. A. Nurani, D. U. C. Rahayu, and H. Haerudin, "Synthesis and characterization hierarchical HY zeolite using template and non template methods," in AIP Conference Proceedings, American Institute of Physics Inc., Oct. 2018. doi: 10.1063/1.5064091.
94. S. M. Seo, D. J. Moon, J. An, H.-K. Jeong, and W. T. Lim, "Time-dependent Ni2+-ion exchange in zeolites y (FAU, si/Al= 1.56) and their single-crystal structures," The Journal of Physical Chemistry C, vol. 120, no. 50, pp. 28563–28574, 2016.
95. Z. Ayad, H. Q. Hussein, and B. A. Al-Tabbakh, "Synthesis and characterization of high silica HY zeolite by basicity reduction," in AIP Conference Proceedings, American Institute of Physics Inc., Mar. 2020. doi: 10.1063/5.0000278.
96. Y. K. Krisnandi et al., "Synthesis and characterization of crystalline NaY-Zeolite from Belitung Kaolin as catalyst for n-Hexadecane cracking," Crystals (Basel), vol. 9, 2019, doi: 10.3390/cryst9080404.
97. Q. Dong, R. Li, and H. Jiao, "Zeolite Catalysts for Selective Hydrocracking of Polycyclic Aromatic Hydrocarbons – Structures and Mechanisms," ChemCatChem, Nov. 2024, doi: 10.1002/cctc.202400117.
98. Y. Khalaf, B. Sherhan, and Z. Shakour, "Hydroisomerization of n-Heptane in a Fixed-Bed Reactor Using a Synthesized Bimetallic Type-HY Zeolite Catalyst," Engineering and Technology Journal, vol. 40, pp. 1–13, Sep. 2022, doi: 10.30684/etj.2022.132491.1124.
99. S. M. Seo, H. S. Kim, D. Y. Chung, J. M. Suh, and W. T. Lim, "The Effect of Co2+-ion exchange time into zeolite y (FAU, Si/Al = 1.56): Their Single-Crystal Structures," Bull Korean Chem Soc, vol. 35, pp. 243–249, Jan. 2014, doi: 10.5012/bkcs.2014.35.1.243.
100. S. Shrestha and P. K. Dutta, "Photochemical water oxidation by manganese oxides supported on zeolite surfaces," ChemistrySelect, vol. 1, no. 7, pp. 1431–1440, 2016.

 doi:10.20944/preprints202512.2606.v1

101. H. S. Kim, D. J. Moon, H. Y. Yoo, J. S. Park, M. Park, and W. T. Lim, "A crystallographic study of Sr2+ and K+ ion-exchanged zeolite Y (FAU, Si/Al = 1.56) from binary solution with different mole ratio of Sr2+ and K+," Journal of Porous Materials, vol. 27, pp. 63–71, Feb. 2020, doi: 10.1007/s10934-019-00783-1.
102. Y. Khabzina, C. Laroche, C. Pagis, and D. Farrusseng, "Monovalent and bivalent cations exchange isotherms for faujasites X and y," Physical Chemistry Chemical Physics, vol. 19, pp. 17242–17249, 2017, doi: 10.1039/c7cp02051a.
103. L. Wu and A. Navrotsky, "Synthesis and thermodynamic study of transition metal ion (Mn2+, Co2+, Cu2+, and Zn2+) exchanged zeolites A and y," Physical Chemistry Chemical Physics, vol. 18, pp. 10116–10122, Apr. 2016, doi: 10.1039/c5cp07918g.
104. M. T. Izquierdo, R. Juan, B. Rubio, and C. Gómez-Giménez, "No removal in the selective catalitic reduction process over Cu and Fe exchanged type Y zeolites synthesized from coal fly ash," Energy Sources, Part A: Recovery, Utilization, and Environmental Effects, vol. 38, no. 9, pp. 1183–1188, 2016.
105. C. Wang, E. Xing, J. Zheng, Y. Luo, and X. Shu, "Effects of Pressured Steaming on the Migration of La3+ Ions and the Performance of As-Prepared LaY Zeolite," Ind Eng Chem Res, vol. 60, no. 47, pp. 17268–17277, 2021.
106. M. Dastanian and F. Seyedeyn-Azad, "Desulfurization of gasoline over nanoporous nickel-loaded Y-type zeolite at ambient conditions," Ind Eng Chem Res, vol. 49, no. 22, pp. 11254–11259, 2010.
107. X. Chen, B. Shen, H. Sun, and G. Zhan, "Ion-exchanged zeolites Y for selective adsorption of methyl mercaptan from natural gas: experimental performance evaluation and computational mechanism explorations," Ind Eng Chem Res, vol. 56, no. 36, pp. 10164–10173, 2017.
108. X. Chen, B. X. Shen, H. Sun, G. X. Zhan, and Z. Z. Huo, "Adsorption and Its Mechanism of CS2 on Ion-Exchanged Zeolites y," Ind Eng Chem Res, vol. 56, pp. 6499–6507, Jun. 2017, doi: 10.1021/acs.iecr.7b00245.
109. P. Tobarameekul, S. Sangsuradet, and P. Worathanakul, "Comparative Study of Zn Loading on Advanced Functional Zeolite NaY from Bagasse Ash and Rice Husk Ash for Sustainable CO2 Adsorption with ANOVA and Factorial Design," Atmosphere (Basel), vol. 13, Feb. 2022, doi: 10.3390/atmos13020314.
110. N. Djeffal, M. Benbouzid, B. Boukoussa, H. Sekkiou, and A. Bengueddach, "CO2 adsorption properties of ion-exchanged zeolite y prepared from natural clays," Mater Res Express, vol. 4, Mar. 2017, doi: 10.1088/2053-1591/aa6465.
111. R. S. Pillai, G. Sethia, and R. V Jasra, "Sorption of CO, CH4, and N2 in alkali metal ion exchanged zeolite-X: grand canonical Monte Carlo simulation and volumetric measurements," Ind Eng Chem Res, vol. 49, no. 12, pp. 5816–5825, 2010.
112. B. Silva et al., "Reutilization of Cr-Y zeolite obtained by biosorption in the catalytic oxidation of volatile organic compounds," J Hazard Mater, vol. 192, no. 2, pp. 545–553, 2011.
113. A. Cauvel, D. Brunel, F. Di Renzo, P. Moreau, and F. Fajula, "Functionalization of Y zeolites with organosilane reagents," in Studies in Surface Science and Catalysis, vol. 94, Elsevier, 1995, pp. 286–293.
114. W. Peng et al., "Grafting of R4N+-Bearing Organosilane on Kaolinite, Montmorillonite, and Zeolite for Simultaneous Adsorption of Ammonium and Nitrate," Int J Environ Res Public Health, vol. 19, no. 19, p. 12562, 2022.
115. R. E. Kukwa and S. E. Dann, "Grafted zeolites for the removal of metal cations from crude oil hydrotreatment extract," Desalination Water Treat, vol. 153, pp. 136–144, Jun. 2019, doi: 10.5004/dwt.2019.23881.
116. H. Sanaeepur, A. Kargari, and B. Nasernejad, "Aminosilane-functionalization of a nanoporous Y-type zeolite for application in a cellulose acetate based mixed matrix membrane for CO 2 separation," RSC Adv, vol. 4, no. 109, pp. 63966–63976, 2014.
117. S. C. Lu, T. Wichidit, T. Narkkun, K. L. Tung, K. Faungnawakij, and C. Klaysom, "Aminosilane-Functionalized Zeolite Y in Pebax Mixed Matrix Hollow Fiber Membranes for CO2/CH4 Separation," Polymers (Basel), vol. 15, Jan. 2023, doi: 10.3390/polym15010102.
118. B. Zhang, K. Zhang, Z. Duan, J. Zhu, and J. Gao, "Y Zeolites Modified by Organosilane for Toluene Adsorption under High Humidity Condition," Am J Analyt Chem, vol. 14, pp. 451–466, 2023, doi: 10.4236/ajac.2023.1410026.

 doi:10.20944/preprints202512.2606.v1

119. L. Yang et al., "Facilely Grafting Small Amine Molecules into Co-Exchanged Zeolite for Enhancing CO2 Adsorption," Ind Eng Chem Res, vol. 63, pp. 5863–5870, Apr. 2024, doi: 10.1021/acs.iecr.3c04422.
120. Y. Li et al., "Grafting of functional organic ligand on zeolite Y for efficient CH4/N2 separation," Sep Purif Technol, vol. 354, p. 128719, 2025.
121. C. Wang et al., "Preparation of amino functionalized hydrophobic zeolite and its adsorption properties for chromate and naphthalene," Minerals, vol. 8, Apr. 2018, doi: 10.3390/min8040145.
122. M. S. Rahaman et al., "Hydrophobic functionalization of HY zeolites for efficient conversion of glycerol to solketal," Appl Catal A Gen, vol. 592, Feb. 2020, doi: 10.1016/j.apcata.2019.117369.
123. H.-T. Vu, F. M. Harth, and N. Wilde, "Silylated zeolites with enhanced hydrothermal stability for the aqueous-phase hydrogenation of levulinic acid to γ-valerolactone," Front Chem, vol. 6, p. 143, 2018.
124. C. Kim, H. S. Cho, S. Chang, S. J. Cho, and M. Choi, "An ethylenediamine-grafted y zeolite: A highly regenerable carbon dioxide adsorbent: Via temperature swing adsorption without urea formation," Energy Environ Sci, vol. 9, pp. 1803–1811, May 2016, doi: 10.1039/c6ee00601a.
125. Y. Guo, J. Qi, F. Wang, B. Fan, W. Hao, and R. Li, "Migration of Framework Aluminum and Tunable Acidity in Y Zeolite by Post-treatment," Ind Eng Chem Res, vol. 62, no. 26, pp. 9951–9960, 2023.
126. A. N. Khazipova, O. S. Travkina, M. R. Agliullin, I. N. Pavlova, B. I. Kutepov, and V. A. Dyakonov, "Modification of the Physicochemical Properties of High-Crystallinity Granular Y Zeolite by Steam Heating and Acid Treatment," Petroleum Chemistry, vol. 61, pp. 284–291, 2021.
127. M. Moosavifar and L. Fathyunes, "Influence of the post-synthesis method on the number and size of secondary mesoporous structure of NaY zeolite and its effect on catalyst loading. An efficient and eco-friendly catalyst for synthesis of xanthenes under conventional heating," Journal of the Iranian Chemical Society, vol. 13, no. 11, pp. 2113–2120, 2016.
128. S. Roy, A. Bhaskaran, and P. C. Meenu, "Microwave-assisted Synthesis of Porous Materials," 2023.
129. T. Le, T. Wang, A. V Ravindra, Y. Xuxiang, S. Ju, and L. Zhang, "Fast synthesis of submicron zeolite Y using microwave heating," Kinetics and Catalysis, vol. 62, no. 3, pp. 436–444, 2021.
130. T. Le, Q. Wang, B. Pan, A. V Ravindra, S. Ju, and J. Peng, "Process regulation of microwave intensified synthesis of Y-type zeolite," Microporous and Mesoporous Materials, vol. 284, pp. 476–485, 2019.
131. S. Abdulridha et al., "A comparative study on mesoporous Y zeolites prepared by hard-templating and post-synthetic treatment methods," Appl Catal A Gen, vol. 612, p. 117986, 2021.
132. M. Zhu, X. An, T. Gui, T. Wu, Y. Li, and X. Chen, "Effects of ion-exchange on the pervaporation performance and microstructure of NaY zeolite membrane," Chin J Chem Eng, vol. 59, pp. 176–181, Jul. 2023, doi: 10.1016/j.cjche.2022.12.006.
133. H. Khan, A. S. Yerramilli, A. D'Oliveira, T. L. Alford, D. C. Boffito, and G. S. Patience, "Experimental methods in chemical engineering: X-ray diffraction spectroscopy—XRD," Can J Chem Eng, vol. 98, no. 6, pp. 1255–1266, 2020.
134. N. Salahudeen and A. S. Ahmed, "Synthesis of hexagonal zeolite Y from Kankara kaolin using a split technique," J Incl Phenom Macrocycl Chem, vol. 87, pp. 149–156, 2017.
135. N. Taufiqurrahmi, A. R. Mohamed, and S. Bhatia, "Nanocrystalline zeolite Y: synthesis and characterization," in IOP Conference Series: Materials Science and Engineering, IOP Publishing, 2011, p. 012030.
136. A. Ul-Hamid, A beginners' guide to scanning electron microscopy, vol. 1. Springer, 2018.
137. N. Kaur, "Transmission Electron Microscopy: A Powerful and Novel Scientific Technique with Nanoscale Resolution for Characterization of Materials," in Microscopic Techniques for the Non-Expert, Springer, 2022, pp. 201–226.
138. R. L. Volkov, V. N. Kukin, P. A. Kots, I. I. Ivanova, and N. I. Borgardt, "Complex pore structure of mesoporous zeolites: unambiguous TEM imaging using platinum tracking," ChemPhysChem, vol. 21, no. 4, pp. 275–279, 2020.
139. Q. Huang et al., "Synthesis of the Y nanometer zeolites from fly ash and its adsorption models for aqueous Cs+ ions," J Radioanal Nucl Chem, vol. 323, no. 1, pp. 65–72, 2020.

 doi:10.20944/preprints202512.2606.v1

140. F. S. Irwansyah et al., "How to read and determine the specific surface area of inorganic materials using the Brunauer-Emmett-Teller (BET) method," ASEAN Journal of Science and Engineering, vol. 4, no. 1, pp. 61–70, 2024.
141. M. Zheng, Y. Chu, Q. Wang, Y. Wang, J. Xu, and F. Deng, "Advanced solid-state NMR spectroscopy and its applications in zeolite chemistry," Prog Nucl Magn Reson Spectrosc, vol. 140, pp. 1–41, 2024.
142. S. Askarli et al., "Influence of Extra-Framework Aluminum Species on the Catalytic Properties of Acidic USY Zeolite in (Hydro) cracking Reactions," ACS Catal, vol. 14, no. 18, pp. 13630–13639, 2024.
143. M. Król, A. Koleżyński, and W. Mozgawa, "Vibrational spectra of zeolite Y as a function of ion exchange," Molecules, vol. 26, no. 2, p. 342, 2021.
144. A. Orlando et al., "A comprehensive review on Raman spectroscopy applications," Chemosensors, vol. 9, no. 9, p. 262, 2021.
145. H. T. Vu, M. Goepel, and R. Gläser, "Improving the hydrothermal stability of zeolite Y by La3+cation exchange as a catalyst for the aqueous-phase hydrogenation of levulinic acid," RSC Adv, vol. 11, pp. 5568–5579, Jan. 2021, doi: 10.1039/d0ra08907a.
146. M. Li et al., "Insight into the Key Role of Yttrium Modification for the Enhanced Hydrothermal Stability over Y-Cu-SSZ-39 Zeolite Catalysts," Energy and Fuels, Dec. 2024, doi: 10.1021/acs.energyfuels.4c04022.
147. L. Zhang, Y. Qin, X. Zhang, X. Gao, and L. Song, "Further Findings on the Stabilization Mechanism among Modified y Zeolite with Different Rare Earth Ions," Ind Eng Chem Res, vol. 58, pp. 14016–14025, Aug. 2019, doi: 10.1021/acs.iecr.9b03036.
148. C. Buttersack, A. König, and R. Gläser, "Stability of a highly dealuminated Y-zeolite in liquid aqueous media," Microporous and Mesoporous Materials, vol. 281, pp. 148–160, Jun. 2019, doi: 10.1016/j.micromeso.2019.02.014.
149. Z. Zhu et al., "Insight into tri-coordinated aluminum dependent catalytic properties of dealuminated Y zeolites in oxidative desulfurization," Appl Catal B, vol. 288, p. 120022, 2021.
150. L. Wang, Y. Jiang, J. Huang, and M. Hunger, "Relation between acidity and local structure of dealuminated zeolites y investigated by solid-state NMR spectroscopy," in Chemeca 2011 (39th: 2011: Sydney, NSW), Engineers Australia Barton, ACT, 2011, pp. 550–558.
151. S. Li et al., "Probing the spatial proximities among acid sites in dealuminated HY zeolite by solid-state NMR spectroscopy," The Journal of Physical Chemistry C, vol. 112, no. 37, pp. 14486–14494, 2008.
152. Z. Muhammad, A. Garba, Y. Ibrahim, and A. H. Birniwa, "Synthesis and characterization of zeolite sourced from rice husk lignocellulosic waste ash," ChemSearch Journal, vol. 15, no. 1, pp. 80–85, 2024.
153. F. H. Blindheim and J. Ruwoldt, "The effect of sample preparation techniques on lignin Fourier transform infrared spectroscopy," Polymers (Basel), vol. 15, no. 13, p. 2901, 2023.
154. A. K. Bahgaat, H. E.-S. Hassan, A. A. Melegy, and A. Abdel Karim, "Synthesis and characterization of zeolite-Y from natural clay of Wadi Hagul, Egypt," Egypt J Chem, vol. 63, no. 10, pp. 3791–3800, 2020.
155. H. Azzan, D. Danaci, C. Petit, and R. Pini, "Unary Adsorption Equilibria of Hydrogen, Nitrogen, and Carbon Dioxide on Y-Type Zeolites at Temperatures from 298 to 393 K and at Pressures up to 3 MPa," J Chem Eng Data, vol. 68, no. 12, pp. 3512–3524, 2023.
156. M. K. Singh and A. Singh, "Thermogravimetric analyzer," in Characterization of Polymers and Fibres, Elsevier, 2022, pp. 223–240. doi: 10.1016/b978-0-12-823986-5.00015-4.
157. B. Bensafi, N. Chouat, A. Maziz, and F. Djafri, "Synthesis and Post-synthesis Modification of Zeolite Y for Improved Methanol Adsorption and Coke Formation Resistance," Silicon, vol. 16, no. 15, pp. 5549–5561, 2024.
158. M. Moreno-González, A. E. Palomares, M. Chiesa, M. Boronat, E. Giamello, and T. Blasco, "Evidence of a Cu2+–Alkane Interaction in Cu-Zeolite Catalysts Crucial for the Selective Catalytic Reduction of NO x with Hydrocarbons," ACS Catal, vol. 7, no. 5, pp. 3501–3509, 2017.
159. A. Brückner, "In situ electron paramagnetic resonance: A unique tool for analyzing structure–reactivity relationships in heterogeneous catalysis," Chem Soc Rev, vol. 39, pp. 4673–4684, Nov. 2010, doi: 10.1039/b919541f.
160. V. A. Reyes Villegas et al., "Sonochemical post-synthesis modification of Y zeolite with iron species," Mater Chem Phys, vol. 331, Feb. 2025, doi: 10.1016/j.matchemphys.2024.130199.

 doi:10.20944/preprints202512.2606.v1

161. C. Douvris, T. Vaughan, D. Bussan, G. Bartzas, and R. Thomas, "How ICP-OES changed the face of trace element analysis: Review of the global application landscape," Dec. 2023, Elsevier B.V. doi: 10.1016/j.scitotenv.2023.167242.
162. V. A. Reyes Villegas, J. I. De León Ramirez, L. Pérez-Cabrera, S. Pérez-Sicairos, J. R. Chávez-Méndez, and V. Petranovskii, "Analysis of catalytic sites in FeY zeolite prepared by sono-assisted exchange of iron (II) ions," Microporous and Mesoporous Materials, vol. 380, Dec. 2024, doi: 10.1016/j.micromeso.2024.113306.
163. K. Argaw Shiferaw, J. M. Mathews, E. Yu, E. Y. Choi, and N. H. Tarte, "Sodium Methoxide/Zeolite-Supported Catalyst for Transesterification of Soybean Waste Cooking Oil for Biodiesel Production," Inorganics (Basel), vol. 11, Apr. 2023, doi: 10.3390/inorganics11040163.